




Regulation of monoamine oxidase A (MAO-A) expression, activity, and function in IL-13–stimulated monocytes and A549 lung carcinoma cells

Received for publication, February 7, 2018, and in revised form, July 6, 2018. Published, Papers in Press, July 18, 2018, DOI 10.1074/jbc.RA118.002321

Sukhamoy Dhabal^{‡1}, Pradip Das^{‡1}, Pritam Biswas[‡], Priyanka Kumari[‡], Valentin P. Yakubenko^{§2}, Suman Kundu[§], Martha K. Cathcart[§], Manjari Kundu[¶],  Kaushik Biswas[¶], and Ashish Bhattacharjee^{‡3}

From the [‡]Department of Biotechnology, National Institute of Technology-Durgapur, Mahatma Gandhi Avenue, Durgapur-713209, Burdwan, West Bengal, India, the [§]Department of Cell Biology, Lerner Research Institute, Cleveland Clinic, and Department of Molecular Medicine, Cleveland Clinic Lerner College of Medicine, Case Western Reserve University, Cleveland, Ohio 44195, and the [¶]Division of Molecular Medicine, Bose Institute, Kolkata 700054, West Bengal, India

Edited by Luke O'Neill

Monoamine oxidase A (MAO-A) is a mitochondrial flavoenzyme implicated in the pathogenesis of atherosclerosis and inflammation and also in many neurological disorders. MAO-A also has been reported as a potential therapeutic target in prostate cancer. However, the regulatory mechanisms controlling cytokine-induced MAO-A expression in immune or cancer cells remain to be identified. Here, we show that MAO-A expression is co-induced with 15-lipoxygenase (15-LO) in interleukin 13 (IL-13)-activated primary human monocytes and A549 non-small cell lung carcinoma cells. We present evidence that MAO-A gene expression and activity are regulated by signal transducer and activator of transcription 1, 3, and 6 (STAT1, STAT3, and STAT6), early growth response 1 (EGR1), and cAMP-responsive element-binding protein (CREB), the same transcription factors that control IL-13-dependent 15-LO expression. We further established that in both primary monocytes and in A549 cells, IL-13-stimulated MAO-A expression, activity, and function are directly governed by 15-LO. In contrast, IL-13-driven expression and activity of MAO-A was 15-LO-independent in U937 promonocytic cells. Furthermore, we demonstrate that the 15-LO-dependent transcriptional regulation of MAO-A in response to IL-13 stimulation in monocytes and in A549 cells is mediated by peroxisome proliferator-activated receptor γ (PPAR γ) and that signal transducer and activator of transcription 6 (STAT6) plays a crucial role in facilitating the transcriptional activity of PPAR γ . We further report that the IL-13-STAT6-15-LO-PPAR γ axis is critical for MAO-A expression, activity, and function, including migration and reactive oxygen species generation. Altogether, these results have major implications for the resolution of inflammation and indicate

that MAO-A may promote metastatic potential in lung cancer cells.

Interleukin (IL)⁴ 13 is a Th2 cytokine that is involved in regulating inflammatory responses and is thought to play a major role during asthma and allergic reactions (1). However, IL-13 primarily acts as an anti-inflammatory molecule that activates monocytes/macrophages toward the M2a phenotype leading to the up-regulation of several genes involved in the resolution of inflammation (2–5). Among the most strongly up-regulated genes in IL-13-activated monocytes/macrophages with potential anti-inflammatory properties are 15-lipoxygenase (15-LO) and monoamine oxidase A (MAO-A) (1, 6–10).

During alternative activation of monocytes/macrophages, IL-13 interacts with a specific cell-surface receptor that utilizes the IL-4R α chain, which combines with and signals through IL-13R α 1 (type II IL-4R, receptor for IL-13) (11). The receptor-associated Jaks that are attached to the type II IL-4R and are stimulated by IL-13 treatment include Jak2 and Tyk2 (1). Jak-mediated activation of Stat proteins leads to Stat translocation and DNA binding thus activating transcription of target genes. In addition to Stat tyrosine phosphorylation, Stat transcriptional activity is also enhanced by serine phosphorylation. The involvement of several Ser/Thr kinases, including p38 MAPK, ERK1/2, and PKC δ , in regulating Stat serine phosphorylation and Stat-dependent gene transcription, has already been demonstrated (12–15). Stat proteins dimerize after tyrosine phos-

This work was supported by Ramalingaswami Fellowship (to A. B.) by the Department of Biotechnology, Government of India, and by Research Grant SERB/SR/SO/HS-093/2013 from SERB, Government of India. The authors declare that they have no conflicts of interest with the contents of this article.

This article contains Figs. S1–S7.

¹ Both authors contributed equally to this work.

² Present address: Dept. of Biomedical Sciences, James H. Quillen College of Medicine, East Tennessee State University, Johnson City, TN 37614.

³ To whom correspondence should be addressed: Dept. of Biotechnology, National Institute of Technology, Durgapur-713209, West Bengal, India. Tel.: 91-343-2754036; E-mail: ashish15lo@yahoo.com.

⁴ The abbreviations used are: IL, interleukin; 15-LO, 15-lipoxygenase; MAO-A, monoamine oxidase A; ODN, oligodeoxyribonucleotide; ROS, reactive oxygen species; PPAR γ , peroxisome proliferator-activated receptor- γ ; Jak, Janus kinase; Stat, signal transducer and activator of transcription; CREB, cAMP-responsive element-binding protein; BCS, bovine calf serum; MT, mutated; MTT, 3-(4,5-dimethylthiazol-2-yl)-2,5-diphenyltetrazolium bromide; DMEM, Dulbecco's modified Eagle's medium; EMT, epithelial to mesenchymal transition; HOPE, hydroxyoctadecadienoic acid; HPODE, hydroperoxylinoic acid; HPETE, hydroperoxyeicosatetraenoic acid; H₂DCFDA, 6-carboxy-2',7'-dichlorodihydrofluorescein diacetate, diacetoxymethyl ester; PEI, polyethylenimine; PBM, peripheral blood monocyte; LPS, lipopolysaccharide; IFN, interferon; NHBE, normal human bronchial epithelial; NSCLC, non-small cell lung cancer; FBS, fetal bovine serum; HRP, horseradish peroxidase; co-IP, co-immunoprecipitation; CRE, cAMP-responsive element; AS, antisense; TMB, tetramethylbenzidine.

phorylation by the Src homology 2-phosphotyrosine interaction, which enables the proteins to be efficiently transported to the nucleus and to bind DNA. DNA binding facilitates the interaction of Stat transcription factors with other proteins and enhances the transcriptional efficiency of the Stat-dependent genes. Jak-mediated activation of Stat1, Stat3, and Stat6 seems to be critical during activation of monocytes/macrophages by IL-13 stimulation and significantly contributes to the IL-13-activated gene expression. IL-13 signaling utilizes both IL-4R α -Jak2-Stat3 and IL-13R α 1-Tyk2-Stat1/Stat6 pathways to regulate the expression of some critical inflammatory genes, including *15-LO* and *MAO-A* (1).

15-LO is a lipid-peroxidating enzyme that is substantially induced in human peripheral blood monocytes after IL-4/IL-13 activation. This enzyme is capable of oxygenating polyunsaturated fatty acids like linoleic and arachidonic acids to their corresponding hydroperoxides like (13S)-HPODE and (15S)-HPETE (16, 17), which have been implicated as inflammatory mediators in cell development and in the pathogenesis of various diseases (18–21). In contrast, MAO-A is a catalytically active flavoprotein that catalyzes the oxidative deamination of biogenic and dietary amines like serotonin, dopamine, norepinephrine, and tyramine and converts them into their corresponding aldehydes and reactive oxygen species (ROS) (22–25). This pro-oxidative enzyme is encoded by the X chromosome and is located in the outer mitochondrial membrane and cytosol (26). MAO-A hyperactivity has been shown to be associated with depression, and previous reports implicate MAO-A inhibitors as effective therapeutics against clinical depression and anxiety (27, 28). Previous studies further demonstrated the involvement of MAO-A in neurodegenerative diseases, including Parkinson's and Alzheimer's disease, by inducing oxidative stress-mediated apoptosis (29, 30). MAO-A deficiency and abnormal activity has been associated with impulsive aggressive behavior (31), neuropsychiatric disorders (32), pancreatic beta-cell function (33), and glucose metabolism (34). MAO-A has also been reported as a vital regulator of embryonic brain development (25). In addition to neuroinflammatory syndromes, involvement of MAO-A has been established in the pathogenesis of many cardiovascular disorders. The predominant role of MAO-A has been shown in myocardial injury (35), heart failure (36), cardiac cell apoptosis (37), and vascular wall remodeling (38). Although MAO-A is associated with resolution of inflammation, MAO-A-mediated ROS generation and subsequent oxidative stress could promote inflammation in cardiovascular diseases. The role of MAO-A in promoting or resolving inflammation may rely on the delicate balance of ROS formation and catabolism. Depending on the cellular expression level of MAO-A, this balance is maintained and can influence many pathogenic pathways that are involved in all of these disease conditions. Recent evidence also suggests that increased MAO-A expression is associated with prostate tumor growth and metastasis (39).

Although activation of MAO-A has been reported by IL-13 in monocyte/macrophage system, several monocytic cell lines fail to induce MAO-A expression in response to IL-13 stimulation. In contrast, U937 cells (pro-monocytic, human myeloid leukemia cell line), which exhibit many characteristics of

monocytes and are used as the experimental model to elucidate mechanisms of monocyte and macrophage differentiation, can induce MAO-A expression after IL-13 stimulation. Induction of MAO-A has also been observed in an IL-13-induced non-monocytic cell line, A549 (human lung epithelium carcinoma cell line). The regulatory mechanisms controlling MAO-A gene expression after IL-13 activation have yet to be explored in monocytes/macrophages, pro-monocytic cells like U937 cells, and in A549 lung cancer cells.

In this study, we demonstrated that MAO-A is co-induced with 15-LO in monocytes/macrophages, normal human bronchial epithelial (NHBE) cells, and in the A549 lung epithelial carcinoma cell line in response to IL-13 treatment, but it is neither present nor induced by IL-13 in monocytic cell lines like THP1 or Monomac6. In contrast, only MAO-A but not 15-LO gene is induced by IL-13 in the promyelomonocytic cells like U937. We investigated the mechanisms involved in regulating the expression/activity and function of MAO-A during IL-13-activation, and we presented evidence that Stat6, 15-LO, and PPAR γ are the critical regulators that are involved in controlling MAO-A gene expression and activity in monocytes/macrophages and A549 cells, which further demonstrated the concerted mechanistic effects of these genes during IL-13-activation. However, IL-13-activated MAO-A gene expression/activity in U937 cells is independent of 15-LO showing completely different gene regulation in U937 cells. We further showed that PPAR γ and 15-LO both are directly involved in regulating the function of MAO-A-mediated migration and ROS generation in monocytes/macrophages and in A549 cells after IL-13 activation. Altogether, the IL-13 > STAT6 > 15-LO > PPAR γ signaling pathways for regulating MAO-A gene expression and function add novel insights into the resolution of inflammation and in the progression of lung cancer.

Results

MAO-A co-induces with 15-LO during IL-13 activation of primary monocytes and A549 cells but not in IL-13-activated U937 monocytic cells

In human peripheral blood monocytes, IL-13 up-regulates expression of a variety of gene products (1), and one of the most strongly up-regulated proteins is the lipid-peroxidizing enzyme 15-LO (6). To study the impact of this Th2-cytokine on monocyte cell physiology more comprehensively, the gene expression pattern was checked after culturing the cells in the presence and absence of IL-13. We performed the IL-13 dose-response and IL-13-mediated time-course experiments in primary monocytes and in A549 cells to determine the relative responsiveness in these cells. Previous results from our group and other groups already reported the IL-13-dependent dose response and time course for the measurement of 15-LO at protein and mRNA levels in primary monocytes (7, 12, 40). These results demonstrated the optimal condition for 15-LO mRNA and protein expression levels after 24- and 48-h incubations with 2 nM IL-13. We found similar conditions (48-h stimulation with 2 nM IL-13) for the maximal expression of MAO-A protein both in primary monocytes and in A549 cells (Fig. S1,

Regulation of MAO-A in IL-13-activated cells

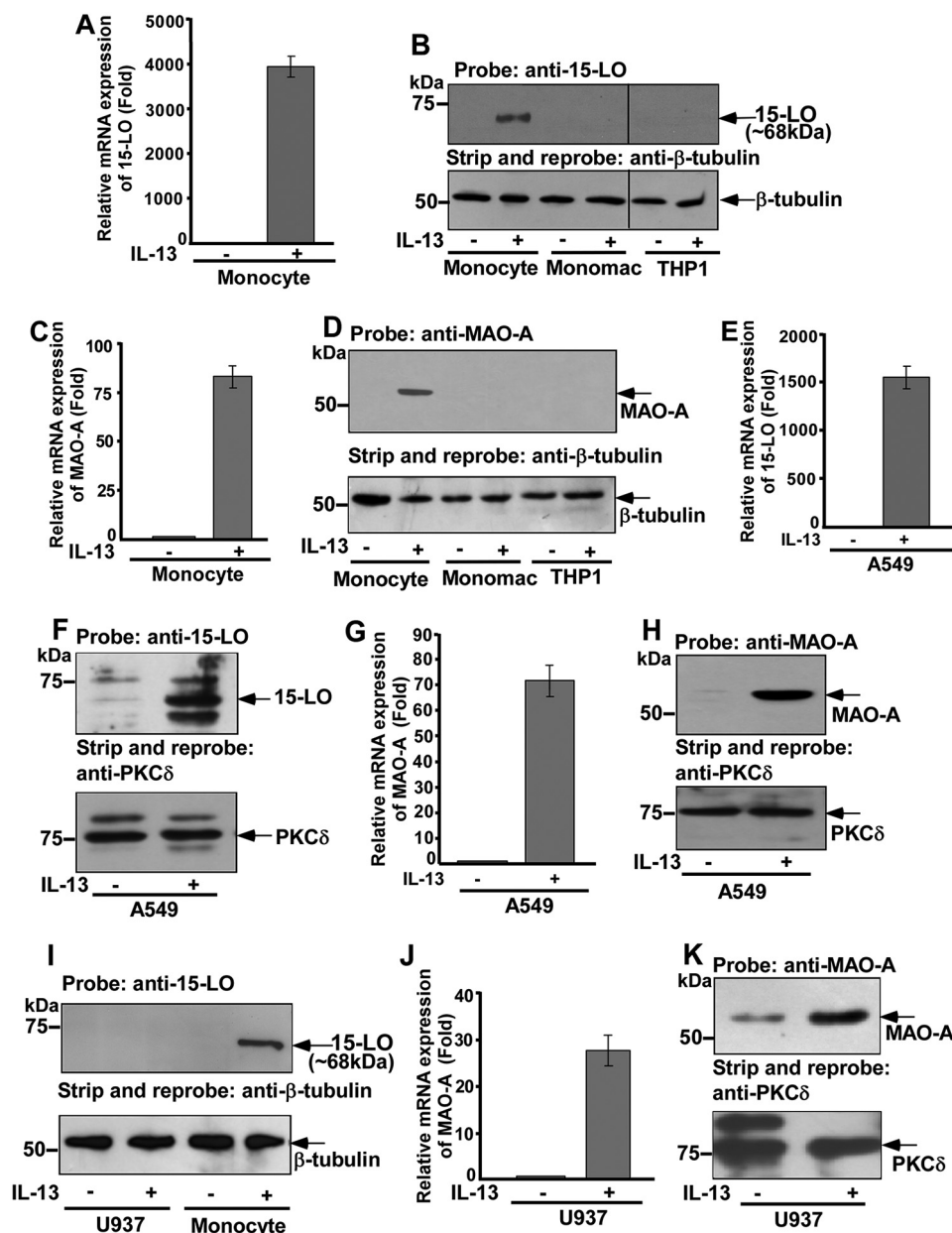


Figure 1. MAO-A is co-induced with 15-LO in primary human monocytes and in A549 cells by IL-13 but not in U937 monocytic cells. Primary blood monocytes, Monomac6, THP1, A549, and U937 cells (5×10^6 /group) were treated with IL-13 (2 nM) for 24 h (mRNA) or 48 h (protein). A, C, E, G, and J, total cellular RNA extracts were prepared and subjected to real-time PCR analysis. After normalization with GAPDH amplification, the fold induction of 15-LO mRNA (A and E) and MAO-A mRNA (C, G, and J) expression for different groups was plotted. Data are the mean \pm S.D. ($n = 3$). For protein expression, cell lysates (50 μ g of postnuclear extracts/lane) were resolved by 10% SDS-PAGE and immunoblotted with antibody against 15-LO (upper panels of B, F, and I) and MAO-A (upper panels of D, H, and K). To confirm equal loading, the blots were then stripped and reprobbed either with β -tubulin (lower panels of B, D, and I) or with PKC δ (lower panels of F, H, and K) antibodies. Arrows indicate the predicted migration of 15-LO, MAO-A, β -tubulin, and PKC δ as determined by the migration of molecular mass markers in the adjacent lanes. Data are from a representative of three repeat experiments showing similar results.

A–D) and for 15-LO protein in A549 cells (Fig. S1E). Following these standardized conditions, we show that 15-LO gene expression is substantially up-regulated in alternatively activated monocytes by IL-13 both at mRNA (more than 4000-fold induction after incubation with IL-13 for 24 h, see Fig. 1A) and at protein levels (after 48 h of IL-13 incubation, see Fig. 1B), whereas IL-13-activated monocytic cell lines such as monomac and THP1 do not show any induction of 15-LO (Fig. 1B). To test whether 15-LO expression is paralleled by augmented MAO-A expression in peripheral blood monocytes, our group further shows that treatment of human peripheral blood monocytes

with IL-13 strongly induces the expression of MAO-A both at the mRNA (around 90-fold induction in response to IL-13 stimulation after 24 h, see Fig. 1C) as well as at the protein level (Fig. 1D). Similar to 15-LO, IL-13 stimulation does not show any induction of MAO-A in monomac and THP1 cells (Fig. 1D). A recent report demonstrated the ability of MAO-A to induce epithelial to mesenchymal transition and thus enhance growth, invasiveness, and metastasis of prostate cancer cells (39), and we tried to investigate whether IL-13 induces MAO-A expression in different other epithelial cancer cells. Our results show that although MAO-A is constitutively present in many of

these cells like HCT116 colorectal cancer cells or PC3 prostate cancer cells (data not shown), co-induction of both 15-LO and MAO-A occurs only in A549 lung epithelial carcinoma cells after IL-13 stimulation both at the mRNA (Fig. 1, E and G, respectively) as well as at the protein level (Fig. 1, F and H, respectively). Because of the inducible nature of MAO-A gene expression in A549 cells (same as monocyte/macrophage system), we continued our studies by testing this specific cell line and tried to uncover the mechanistic details of MAO-A expression after IL-13 stimulation in both monocytes/macrophages as well as in A549 cells.

U937 is a pro-monocytic, human myeloid leukemia cell line that has many common characteristics of monocytes and is extensively used as a model monocytic system to investigate the mechanisms involved in either monocyte-endothelium attachment or the differentiation of pro-monocytes into mature monocytes or into macrophages. Hence, we wanted to identify whether the same regulatory mechanisms for IL-13-driven MAO-A gene expression/activity exist in immature (U937 cells) and in mature monocytes. Our experimental results with U937 cells (promyelomonocytic cell line) show a significant increase of MAO-A mRNA (around 30-fold induction after IL-13 activation for 24 h, see Fig. 1J) and protein levels (after 48 h of incubation with IL-13, see Fig. 1K). Surprisingly, IL-13 failed to induce 15-LO expression in U937 cells after 48 h of IL-13 stimulation (Fig. 1I). These results indicate that IL-13-mediated MAO-A induction parallels 15-LO up-regulation in peripheral blood monocytes and in A549 cells but not in U937 cells, which indicates that regulation of MAO-A gene expression by IL-13 may be correlated with the up-regulation of 15-LO expression in primary monocytes and in A549 cells but may proceed via a 15-LO-independent pathway in U937 cells.

Induction of 15-LO and MAO-A gene expression occurs in alternatively activated monocytes by IL-13 but not in conventionally activated monocytes by LPS or IFN γ

To examine whether 15-LO and MAO-A genes are specifically up-regulated in alternatively activated monocyte/macrophages by IL-13, we conducted several new experiments where we compared our data (in alternatively activated monocyte/macrophages by IL-13) with conventionally activated monocyte/macrophages in response to LPS or IFN γ . Our results, included in Fig. S2, A–D, demonstrate that 15-LO and MAO-A genes are up-regulated in alternatively activated monocyte/macrophages by IL-13 at mRNA (Fig. S2, A and B) and at protein levels (Fig. S2, C and D), although these genes are not expressed or induced in conventionally activated monocyte/macrophages by LPS (Fig. S2, A–D). Further comparative experiments with IFN γ also show that when 15-LO and MAO-A genes (at mRNA level) are induced by IL-13 activation, there is practically very little/no induction of either 15-LO or MAO-A genes after IFN γ stimulation alone or in combination with IL-13 (Fig. S2, E and F). These results thus confirm the significance of the impact of IL-13 on 15-LO or MAO-A in alternatively activated monocyte/macrophages.

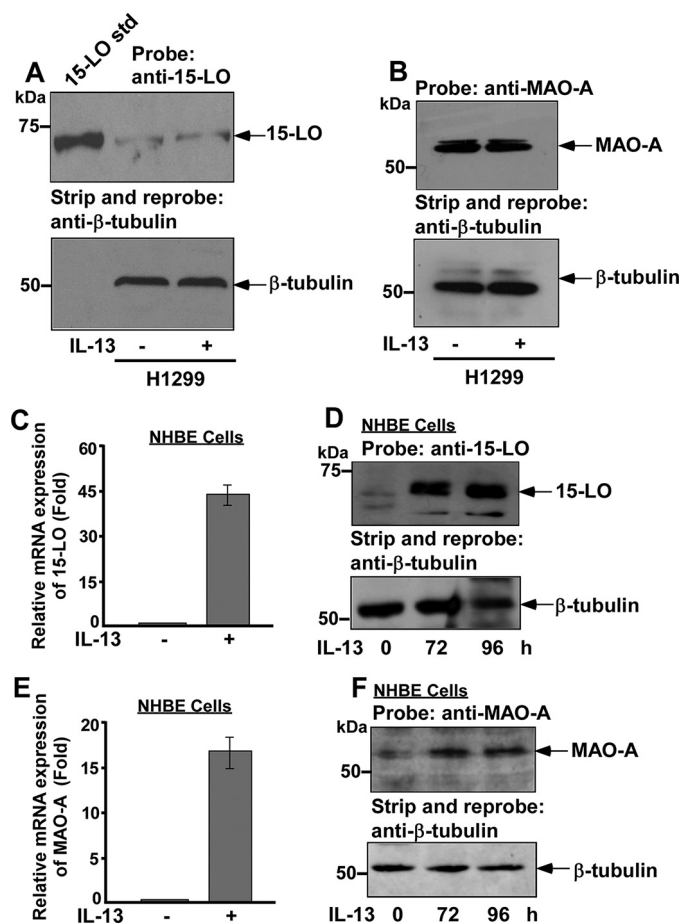


Figure 2. MAO-A is overexpressed in H1299 lung cancer cells and not induced by IL-13, whereas it is co-induced with 15-LO in normal human bronchial epithelial cells after IL-13 stimulation. H1299 non-small cell lung cancer cells and NHBE cells were incubated with IL-13 (2 nm i.e. 30 ng/ml) for 48 h (for H1299 protein), 72 h (for NHBE mRNA), or for the indicated time intervals (for NHBE protein). A, B, D, and F, cell lysates (50 μ g of postnuclear extracts/lane) were resolved by 10% SDS-PAGE and immunoblotted with antibody against 15-LO (upper panels of A and D) and MAO-A (upper panels of B and F). In the upper panel of A, recombinant 15-LO (0.1 μ g) was used as a standard. To confirm equal loading, the blots were then stripped and re-probed with β -tubulin antibody. Arrows indicate the predicted migration of 15-LO, MAO-A, and β -tubulin as determined by the migration of molecular mass markers in the adjacent lanes. C and E, total cellular RNA extracts were prepared and subjected to real-time PCR analysis. After normalization with GAPDH amplification, the fold induction of 15-LO mRNA (C) and MAO-A mRNA (E) expression for different groups was plotted. Data are the mean \pm S.D. ($n = 3$). Data are from a representative of two repeat experiments showing similar results.

MAO-A is constitutively expressed in H1299 NSCLC cells, whereas IL-13 stimulation leads to concordant 15-LO and MAO-A expression in NHBE cells

We further investigated whether in many other epithelial cancer cells like in H1299 NSCLC or in HCT116 colorectal cancer cells, concordant 15-LO and MAO-A induction is present or not following IL-13 stimulation. In H1299 cells, 15-LO expression level is very low and is not induced by IL-13 (Fig. 2A). In contrast, MAO-A is constitutively overexpressed in H1299 cells but is not further induced upon IL-13 stimulation (Fig. 2B). A similar type of constitutive MAO-A overexpression is found in HCT116 cells, and here also the MAO-A level is not induced upon IL-13 activation (data not shown). So these results thus demonstrate that in H1299 NSCLC and in other

Regulation of MAO-A in IL-13-activated cells

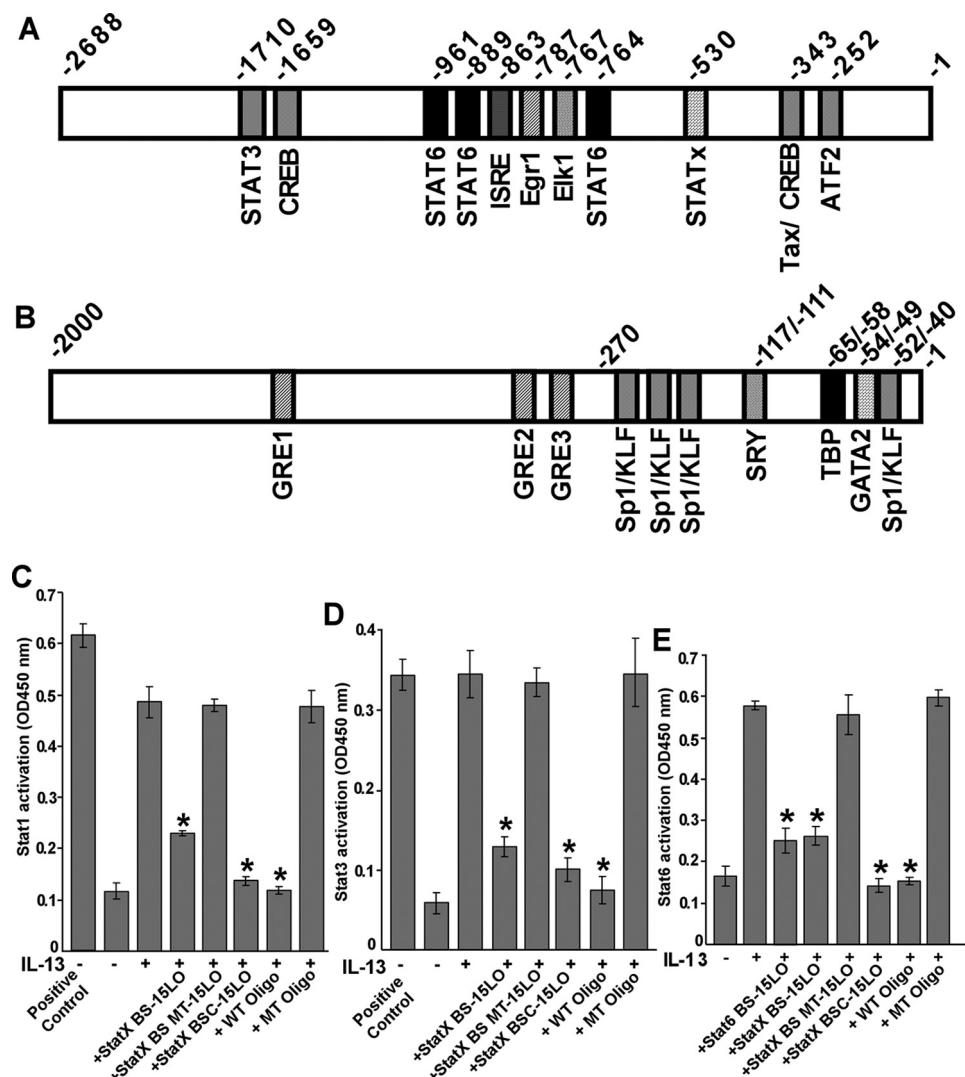


Figure 3. In IL-13-stimulated monocytes, Stats (Stat1, Stat3, and Stat6) bind to their cognate DNA-binding sequences located in the 15-LO promoter. *A*, predicted transcription factor-binding sites of 15-LO upstream sequences. *ISRE*, interferon-stimulated response element; *Elk1*, member of Ets oncogene family; *Tax/CREB*, CREB family member; *ATF2*, activating transcription factor 2, CREB family. *B*, predicted transcription factor-binding sites of MAO-A upstream sequences. *Sp1/KLF*, specificity protein1/Kruppel-like factor; *GATA2*, GATA-binding protein 2; *TBP*, TATA-binding protein; *SRY*, sex regulatory gene on chromosome Y; *GRE1*, -2, and -3, glucocorticoid response elements 1–3. Transcription factor-binding sites are predicted by Genomatix (www.genomatix.de). Upstream sequences for 15-LO, -2688 to -1; upstream sequences for MAO-A, -2000 to -1. *ATG* = +1 to +3. Human monocytes (5×10^6 /group) (*C*, *D*, and *E*) were either untreated or directly stimulated with IL-13 (2 nM) for 1 h. To measure the binding of Stat1 (*C*), Stat3 (*D*), and Stat6 (*E*) to their cognate DNA-binding sequence present in the 15-LO promoter, 5 μ g of nuclear extracts/well were run in triplicate to detect activated Stat1, Stat3, and Stat6 using a TransAM™ Stat family kit. StatX BS-15LO, Stat6 BS-15LO, and StatX BSC-15LO were used as competitors, whereas StatX BS MT-15LO was used as a noncompetitor (see “Results” and “Experimental procedures”). All the competitors and noncompetitors were used at a concentration of 20 pmol/well. Nuclear extracts from IFN γ -stimulated COS-7 cells and IL-6-stimulated HepG2 cells were used as positive controls for activated Stat1 (*C*) and Stat3 (*D*), respectively. The wild-type (*WT*) and mutated (*MT*) consensus oligonucleotides were used to monitor the specificity of the assay. The results are representative of three independent experiments. Data are the mean \pm S.D. ($n = 3$). Significant differences were determined by comparing each group to the IL-13-treated monocytes as the control (*, $p < 0.003$ in *C*, and *, $p < 0.002$ in *D* and *E*).

epithelial cancer cells, MAO-A is already overexpressed, and no further IL-13-dependent induction mechanism exists in these cells.

We also examined NHBE cells for the co-induction of 15-LO and MAO-A in response to IL-13 stimulation. Our results are shown in Fig. 2, *C–F*, and they reveal that after 72 h of incubation with IL-13, 15-LO, and MAO-A, genes are co-induced in NHBE cells at mRNA (Fig. 2, *C* and *E*) and at protein levels (Fig. 2, *D* and *F*), similar to our previous observations in primary monocytes and in A549 lung carcinoma cells. These results thus show the pathophysiological implication of the co-induction of 15-LO and MAO-A and further confirm that the local-

ization of this phenomenon is not restricted only in immune or cancer cells.

Stats (Stat1, Stat3, and Stat6) bind to their cognate sequences derived from the 15-LO promoter in response to IL-13 treatment

As we demonstrated previously that Stat1, Stat3, and Stat6 are all required to control IL-13-mediated 15-LO and MAO-A gene expression (1, 12), we next examined whether the Stats are binding to both 15-LO and MAO-A promoter. To investigate the binding of Stat transcription factors (Stat1, Stat3, and Stat6) to their cognate DNA-binding sites present in the 15-LO pro-

moter (Fig. 3A) after IL-13 stimulation, we performed competitive binding experiments using ELISA-based activation assays for Stat1, Stat3, and Stat6. Our results indicated that the basal level of binding activity of Stats (Stat1, Stat3, and Stat6) to their consensus DNA-binding sequence was enhanced (~4-fold) by IL-13 treatment (Fig. 3, C–E). StatX BS-15LO (oligonucleotides corresponding to the cognate Stat-binding site (StatX binds Stat1, Stat3, or Stat6) in the context of 15-LO promoter-flanking sequences) was used as a competitor in this assay and significantly inhibited the IL-13-induced DNA-binding activity of Stat1 (Fig. 3C, *, $p < 0.003$), Stat3 (Fig. 3D, *, $p < 0.002$), and Stat6 (Fig. 3E, *, $p < 0.002$). For competitive binding, Stat6 BS-15LO (oligonucleotides corresponding to one of the cognate Stat6-binding sites (–961) in the context of flanking sequences present in the 15-LO promoter) was also added prior to addition of the nuclear extract. Stat6 BS-15LO significantly attenuated the IL-13-induced Stat6 DNA-binding activity (*, $p < 0.002$) (Fig. 3E). StatX BSC-15LO (oligonucleotides containing the consensus Stat-binding site in the context of the same flanking sequences present in StatX BS-15LO) was also used as a competitor for comparison. Addition of StatX BSC-15LO in this assay profoundly inhibited IL-13-stimulated 15-LO DNA-binding activity of Stat1, Stat3, and Stat6 (Fig. 3, C–E). The wild-type (WT) consensus oligonucleotides also significantly reduced DNA-binding activity of Stat1, Stat3, and Stat6 (Fig. 3, C–E). Conversely, StatX BS MT-15LO (a mutated sequence of the cognate Stat-binding site in the context of the same flanking sequences present in StatX BS-15LO) and the MT consensus oligonucleotides were used as noncompetitors in this assay and caused essentially no inhibition of IL-13-induced DNA-binding activity of Stats (Stat1, Stat3, and Stat6) (Fig. 3, C–E). These data show the direct binding of Stat transcription factors (Stat1, Stat3, and Stat6) to their cognate DNA-binding sites in the context of flanking sequences present in the 15-LO promoter after IL-13 stimulation in primary monocytes.

In contrast, our predicted transcription factor-binding sites of MAO-A upstream sequences do not reveal any Stat consensus binding site in the MAO-A promoter but show the presence of multiple Sp1-, GATA2-, TBP-, and GRE-binding sites (Fig. 3B). To justify and validate the prediction of different transcription factor-binding sites located in the MAO-A promoter, we pursued a control experiment to determine whether the Sp1 transcription factor binds with the cognate binding sequence present in the MAO-A promoter. Our results demonstrated that the basal level of DNA-binding activity of Sp1 to the cognate binding sequence located in MAO-A gene promoter was increased substantially in the presence of IL-13 (more than 4-fold) (Fig. S3). Sp1BS1-MAO-A and Sp1 BS2-MAO-A, oligonucleotides corresponding to the cognate Sp1-binding sites in the context of MAO-A promoter flanking sequences, were used as competitors in this assay, and significantly reduced the IL-13-stimulated DNA-binding activity of Sp1 (Fig. S3, *, $p < 0.005$). Sp1BS2C-MAO-A (oligonucleotides containing the consensus Sp1-binding site in the context of the same flanking sequences present in Sp1BS2-MAO-A) was also used as a competitor for comparison. Sp1BS2C-MAO-A significantly inhibited IL-13-induced DNA-binding activity of Sp1 (Fig. S3). The wild-type (WT) consensus oligonucleotides also profoundly

inhibited Sp1 activation. In contrast, Sp1BS2 MT-MAO-A (a mutated sequence of the cognate Sp1-binding site in the context of the same flanking sequences present in Sp1BS2-MAO-A) and the MT consensus oligonucleotides were used as noncompetitors in this assay and showed no inhibitory effect on IL-13-stimulated DNA-binding activity of Sp1 (Fig. S3). These data thus validate our *in silico* predicted analysis and present evidence that in response to IL-13 stimulation, Sp1 transcription factor directly binds to the cognate DNA-binding sites (as predicted by our present analysis) in the MAO-A promoter after IL-13 stimulation in primary monocytes.

Egr-1 and CREB transcription factors regulate IL-13-activated MAO-A gene expression in primary human monocytes

We previously demonstrated that in primary human monocytes Egr-1 (early growth response-1) and CREB specifically bind to their cognate sequences located at the 15-LO promoter in response to IL-13 stimulation (15). Our data provided further evidence about the existence of two distinct bifurcating parallel signaling pathways downstream of the IL-13 receptor that regulates 15-LO gene expression in primary monocytes (15). We revealed that other than the canonical IL-4R α -Jak2-Stat3-dependent pathway (14), there exists an IL-13R α 1-Tyk2-mediated pathway that is required for IL-13-induced Egr-1 and CREB activation via MEK-ERK1/2 and thereby implicated transcription factors Egr-1 and CREB as critical regulators of IL-13-induced 15-LO gene expression in primary human monocytes (15). As 15-LO and MAO-A genes are co-induced upon exposure to IL-13 during alternative activation of monocytes, we further investigated the role of Egr-1 and CREB transcription factors in regulating IL-13-stimulated MAO-A gene expression in primary monocytes. To show the impact of these transcription factors on MAO-A gene expression, we transfected monocytes with decoy ODNs specific for Egr-1 and CREB consensus sequences for 24 h and stimulated with IL-13 for an additional 24 or 48 h. We then determined the mRNA and protein expression levels of MAO-A by comparing with monocytes transfected with scrambled decoy ODN using quantitative real time PCR and Western blot analysis (Fig. S4, A and B).

As demonstrated in Fig. S4A, transfection of monocytes with Egr-1 and CREB decoy ODNs significantly inhibited IL-13-induced MAO-A mRNA expression levels as compared with monocytes transfected with scrambled decoy ODN (44% for Egr-1 and 59% for CREB). Co-transfection with a combination of both Egr-1 and CREB decoy ODNs (2 μ M each) down-regulated MAO-A mRNA levels even further (85% inhibition with the combination) as compared with the scrambled decoy ODN-transfected group. Transfection of monocytes in the absence of the decoy ODNs (transfection control) as well as in the presence of the scrambled decoy ODNs followed by IL-13 stimulation showed very little effect on MAO-A protein expression as compared with the nontransfected monocytes induced by IL-13 (Fig. S4B). However, similar to the MAO-A mRNA, both Egr-1 and CREB decoy ODNs individually attenuated IL-13-activated MAO-A protein expression in a substantial manner (Fig. S4B). Co-transfection of Egr-1 and CREB decoy ODNs (1 μ M each) also inhibited the IL-13-stimulated MAO-A protein

Regulation of MAO-A in IL-13-activated cells

expression significantly as compared with scrambled decoy ODN-transfected monocytes (Fig. S4B). We estimated the effect of transfection of these decoys quantitatively as compared with scrambled decoy ODNs, and the results are represented in Fig. S4C. Our results reveal that transfection of the Egr-1 decoy and CREB decoy inhibited IL-13-induced MAO-A protein expression by ~35 and ~42%, whereas the combination of Egr-1 and CREB decoy ODNs (1 μ M each) reduced IL-13-stimulated MAO-A protein expression by ~67% compared with the scrambled decoy ODN-transfected monocytes (Fig. S4C). These data thus strongly support the regulatory role of transcription factors Egr-1 and CREB in mediating IL-13-stimulated MAO-A gene expression in primary monocytes probably by inducing 15-LO expression.

Stats (Stat1, Stat3, and Stat6), Egr-1, and CREB transcription factors are involved in maintaining MAO-A enzyme activity in IL-13-stimulated monocytes

Earlier we showed that Stat1, Stat3, and Stat6 are all required for 15-LO as well as MAO-A gene expression in alternatively activated monocytes/macrophages by IL-13 (1, 12). We further demonstrated that Egr-1 and CREB transcription factors also regulate 15-LO (15) and MAO-A (Fig. S4) gene expression in IL-13-activated monocytes. Here, we investigated the role of these transcription factors in controlling the MAO-A enzyme activity in monocytes after IL-13 stimulation. To examine that, we transfected primary monocytes with the decoy ODNs of all of these transcription factors along with the mismatch/scrambled decoy ODN controls followed by IL-13 stimulation, and we then performed the native MAO-A enzyme activity assay. Our results show that all the Stat decoys markedly attenuated MAO-A enzymatic activity in IL-13-activated monocytes (*, $p < 0.002$), whereas the mismatched ODNs of Stat1/Stat3 and Stat6 scramble (used as controls) had very little effect on IL-13-stimulated MAO-A enzyme activity (Fig. 4A). To check the specificity of this assay, we treated monocytes with the MAO-A-specific antisense or control sense ODNs before IL-13 stimulation. Treatment of MAO-A-specific antisense substantially inhibited the MAO-A enzymatic activity, whereas the sense control is without effect (Fig. 4A).

A similar experiment performed using Egr-1 and CREB decoy ODNs again shows that these transcription factors also down-regulated the IL-13-induced MAO-A activity both individually as well as in combination, whereas the scrambled decoy ODNs had no effect (Fig. 4C). Here, the specificity of the enzymatic assay was also confirmed by using the MAO-A antisense treatment (Fig. 4C). To examine the effectiveness of transfection using the decoy ODNs and mismatched/scrambled decoy ODNs, we performed ELISA-based DNA-binding activity assay of the transcription factors. Our results shown in Fig. 4, B and D, demonstrate that decoy ODNs of the transcription factors (Stat1, Stat3, Stat6, Egr-1, and CREB) significantly reduce the DNA-binding activity of the corresponding transcription factors, whereas the mismatched/scrambled decoy ODNs have no inhibitory effect compared with the transfection control groups.

To check the transfection efficiency and equivalency across multiple biological replicates using the decoy/mismatched

decoy ODNs, we performed co-transfection experiments in monocytes by mixing 2 μ g of pmaxGFP with each group containing 2 μ M Stat1 and Stat3 decoy ODNs or mismatched decoy ODNs (as they are not tagged with a reporter of expression like GFP). After the co-transfection, monocytes were kept in 10% BCS/DMEM for 24 h and were observed under bright field and fluorescence. From the results of this experiment (Fig. S5A), we calculated the transfection efficiency for different biological replicates, and our data show that the transfection efficiency for different groups varies, ranging from a mean value of 46–50% (as presented in Fig. S5B). These data demonstrate more or less an equivalent level of transfection across multiple biological replicates. We further show evidence of approximately equal levels of GFP expression in different groups as shown in Fig. S5C.

Therefore, the results presented in Fig. 4 suggest that Stats (Stat1, Stat3, and Stat6) as well as Egr-1 and CREB transcription factors are critical regulators of MAO-A expression/enzyme activity in alternatively activated monocytes by IL-13.

IL-13-induced MAO-A gene expression in alternatively activated monocytes/macrophages and in A549 cells is 15-LO-dependent

As 15-LO and MAO-A are co-induced upon IL-13 exposure in monocytes/macrophages and in A549 cells, and because both of them are regulated by the transcriptional activation of several Stats (Stat1, Stat3, and Stat6), Egr-1, and CREB in the monocyte/macrophage system, we further investigated whether one of them is the upstream regulator of another. Hence, we treated monocytes with the activity inhibitors of both 15-LO and MAO-A and assessed their effect on MAO-A and 15-LO expression, respectively, at mRNA levels after IL-13 stimulation. Our results show that pretreatment with selective 15-LO activity inhibitor PD146176 reduces the mRNA expression of MAO-A in IL-13-activated monocytes significantly in a dose-dependent manner, whereas pretreatment of monocytes with MAO-A-specific inhibitor moclobemide has no inhibitory effect on IL-13-induced 15-LO mRNA levels (Fig. S6, A and B). These results thus indicate 15-LO as the upstream regulator of MAO-A. To confirm the direct involvement of 15-LO as the upstream regulator of MAO-A gene expression, we first examined the effect of 15-LO antisense ODN on 15-LO expression at both the mRNA and protein level. Cells were treated with the 15-LO-specific antisense or control sense ODN as described earlier (41) and then stimulated with IL-13. Total cellular RNA or proteins were extracted for real time RT-PCR or Western blot analysis. Our results reveal that the 15-LO-specific antisense ODN significantly inhibited both the IL-13-induced 15-LO mRNA in A549 cells and in primary monocytes (Fig. 5, A and C, respectively) (*, $p < 0.005$) and 15-LO protein expression in monocytes (Fig. 5E), whereas the 15-LO sense ODN showed no effect (Fig. 5, A, C, and E). To demonstrate the direct involvement of 15-LO in IL-13-activated MAO-A gene expression, monocytes were treated with 15-LO-specific antisense or sense ODNs and then stimulated with IL-13. IL-13-induced MAO-A mRNA expression was significantly attenuated by 15-LO antisense ODN (*, $p < 0.005$) in both A549 cells as well as in primary monocytes (Fig. 5, B and D, respectively),

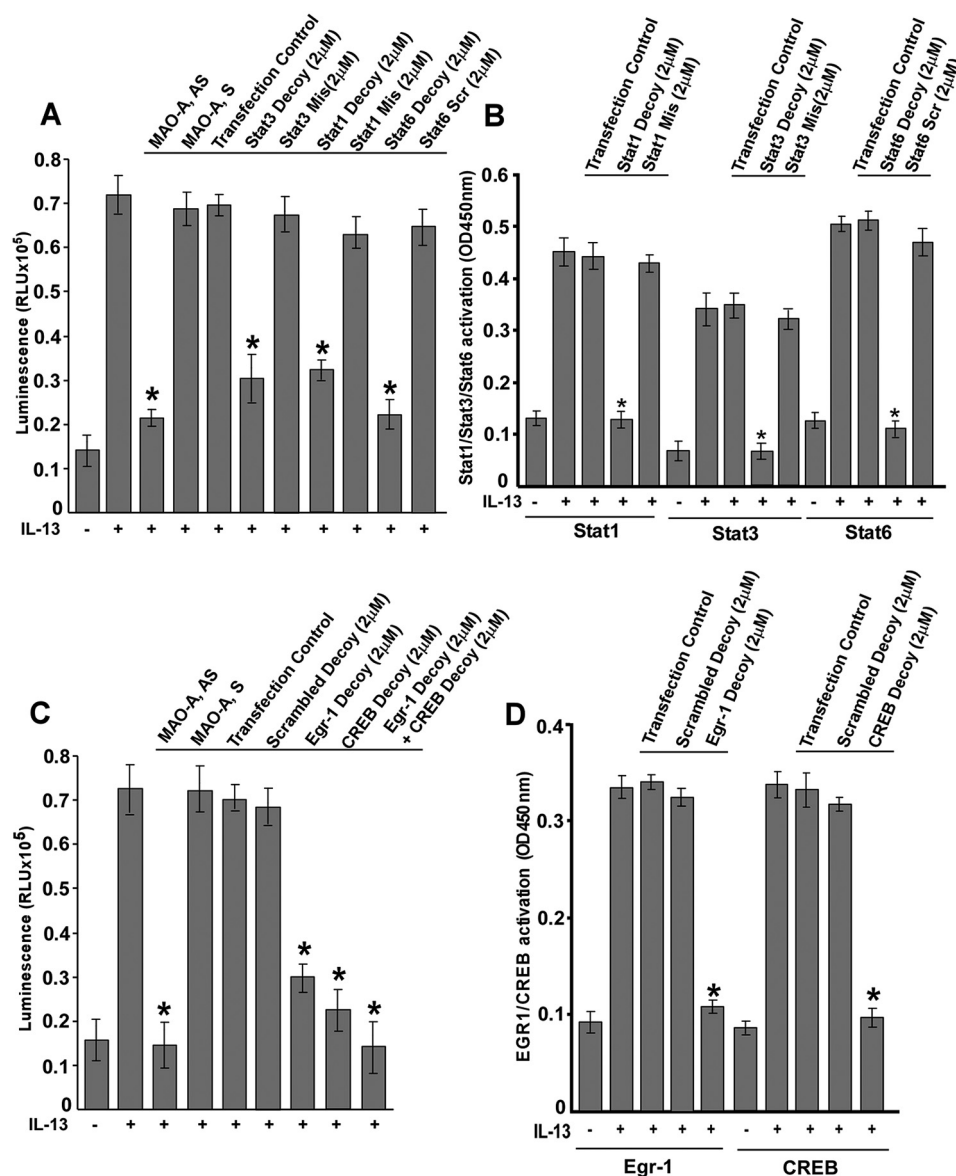


Figure 4. Stats (Stat1, Stat3, and Stat6), Egr-1, and CREB transcription factors regulate MAO-A activity via 15-LO expression in alternatively activated monocytes/macrophages by IL-13. Monocytes (5×10^6 /group) were either transfected with or without decoy or mismatched (*Mis*)/scrambled (*Scr*) decoy ODNs to Stat3, Stat1, and Stat6 (A) or with 2 μM scrambled, Egr-1, or CREB decoy ODNs or a combination of both Egr-1 and CREB decoy ODNs at 2 μM (C) for 24 h prior to the addition of IL-13 (A and C) for 48 h. In some groups, monocytes (5×10^6 /group) were pre-treated with MAO-A sense (S) or antisense (AS) ODN (A and C) and incubated with IL-13 (2 nm) for 48 h. A and C, native MAO-A enzyme activity was detected. In a total volume of 50 μl , 20 μl of whole-cell extract was incubated with substrate (final concentration, 40 μM) in the presence of MAO reaction buffer (100 mM HEPES (pH 7.5); 5% glycerol). After incubation at room temperature for 3 h, 50 μl of luciferin detection reagent was added, and the luminescent signal was measured after 20 min. To show the effect of decoy ODNs of Stats (Stat1, Stat3, and Stat6), Egr-1, and CREB on IL-13-induced DNA-binding activity of the corresponding transcription factors, ELISA-based DNA-binding activity assay was performed and represented in B and D. Data represented as mean \pm S.D.; ($n = 3$, $p < 0.002$). Data in A–D are from a representative of three independent experiments.

whereas the 15-LO sense ODN showed no inhibitory effect. Similar to MAO-A mRNA, MAO-A protein expression was also checked after treatment with 15-LO antisense or sense ODNs followed by incubation with IL-13. 15-LO antisense substantially inhibited the IL-13-induced expression of MAO-A protein in primary monocytes, whereas 15-LO sense ODN had no inhibitory effect (Fig. 5F). The effect of 15-LO antisense on both the IL-13-stimulated expression of 15-LO and MAO-A was further quantitatively determined and represented in Fig. 5, G and H, respectively, based on the densitometric analysis of the results shown in Fig. 5, E and F. Our data showed that 15-LO antisense almost completely inhibited the expression of 15-LO

protein (Fig. 5G), whereas it reduced the expression of the MAO-A protein level by $\sim 70\%$ compared with the IL-13-treated control group (Fig. 5H). These results confirm that the suppression of IL-13-stimulated 15-LO expression is directly related with the down-regulation of MAO-A expression in monocytes and in A549 cells. To further assess the specificity of our antisense-based results, we checked whether any other important marker during alternative activation of monocytes by IL-13 is also attenuated by the treatment of 15-LO antisense ODNs in monocytes. To investigate that, we analyzed the effect of 15-LO-specific antisense ODN treatment on the expression of mannose receptor, a universal marker of alternative

Regulation of MAO-A in IL-13-activated cells

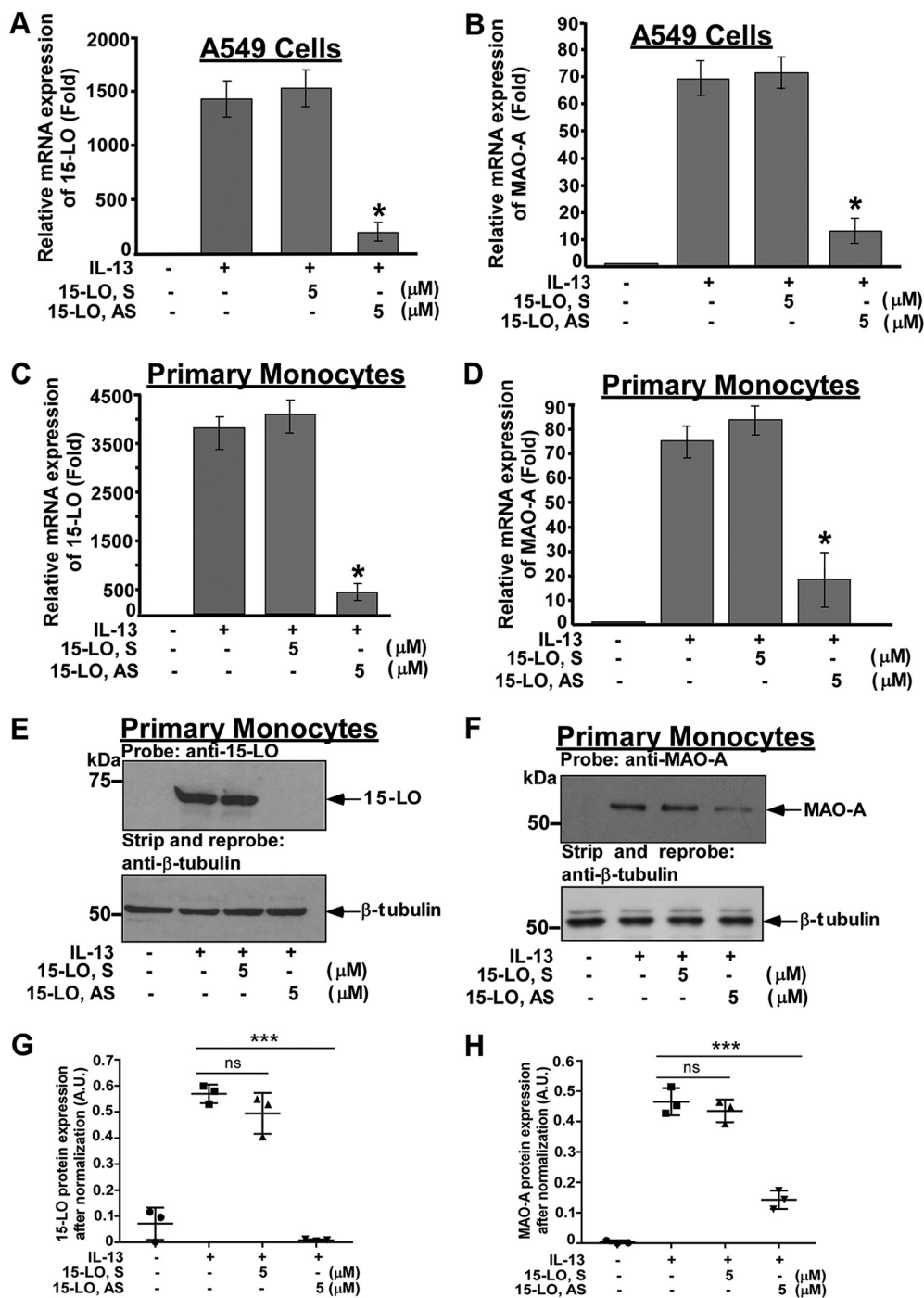


Figure 5. 15-LO regulates IL-13-activated MAO-A gene expression in primary monocytes and in A549 cells. Primary monocytes and A549 cells (5×10^5 /group) were either pretreated with 15-LO antisense (AS) or sense (S) ODNs ($5 \mu\text{M}$) (A–F) for 48 h followed by stimulation with IL-13 either for 24 h (mRNA) or for 48 h (protein). A–D, total cellular RNA extracts were prepared and subjected to real-time PCR analysis. After normalization with GAPDH amplification, the fold induction of 15-LO (A and C) and MAO-A (B and D) mRNA expression for different groups was plotted. Data are the mean \pm S.D. ($n = 3$). *, $p < 0.005$ compared with the IL-13-treated group. E and F, the post-nuclear extracts were separated by 8% SDS-PAGE and immunoblotted with 15-LO- (upper panel of E) and MAO-A (upper panel of F)-specific antibodies. The same blots were stripped and reprobed with β -tubulin antibody to assess equal loading (lower panels of E and F). The data shown represent one of three separate experiments giving similar results. G and H, the densitometric quantification of 15-LO and MAO-A protein expression of monocytes was detected post-transfection with 15-LO sense (S) and antisense (AS) ODNs as indicated using ImageJ software. The data were shown after normalization with the β -tubulin levels and represented in A.U., i.e. arbitrary units. Data are the means \pm S.E. and from three separate experiments as mentioned earlier. Significant differences were determined by comparing the sense and antisense treated groups to the IL-13-treated control (***, $p < 0.001$).

monocyte/macrophage activation (3, 42, 43). Primary monocytes were pretreated with 15-LO-specific antisense and sense ODNs before stimulation with IL-13. After 5 days of incubation, the expression of the mannose receptor was evaluated by

FACS analysis and was substantially increased by IL-13 stimulation (Fig. S6C), but the 15-LO-specific antisense ODN showed no effect on IL-13-stimulated up-regulation of mannose receptor expression (Fig. S6C). These results thus confirm

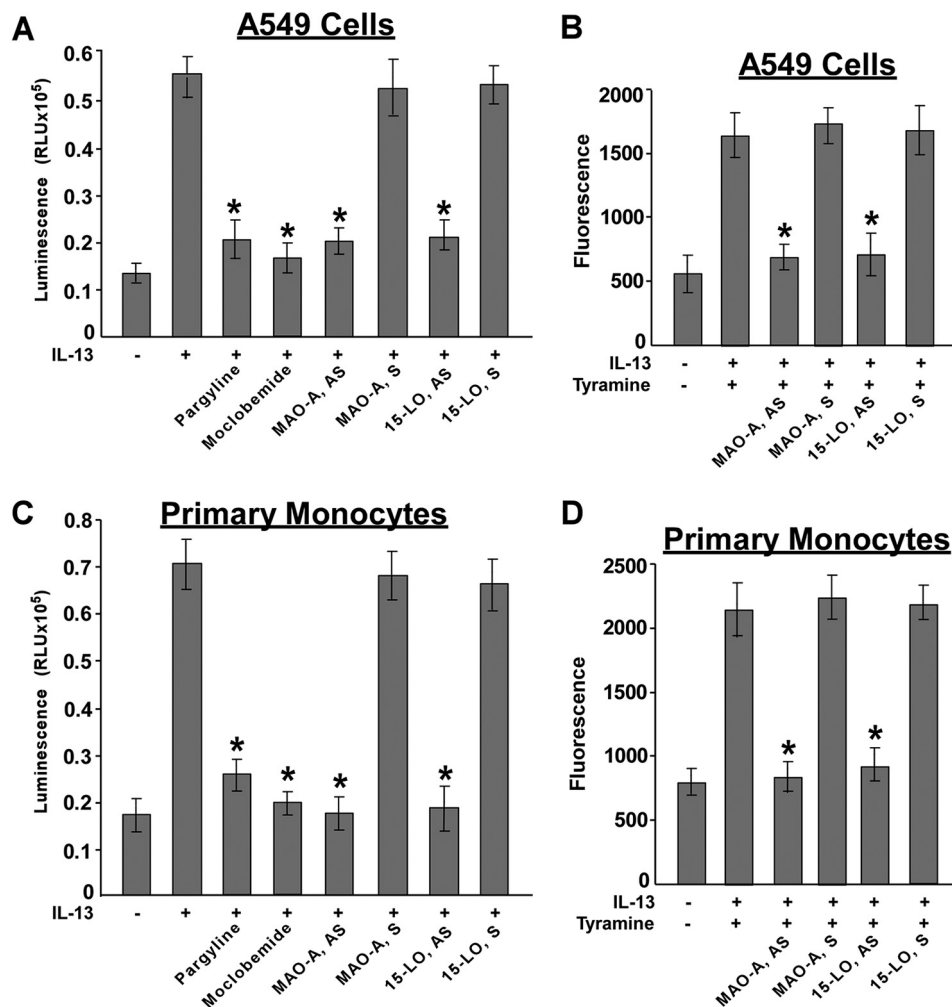


Figure 6. 15-LO is directly involved in regulating MAO-A enzyme activity in IL-13-stimulated A549 cells and primary monocytes/macrophages. Monocytes and A549 cells (5×10^6 /group) were either pre-treated with MAO-A and 15-LO sense (S) or antisense (AS) ODNs (A–D) and incubated with IL-13 (A–D) (2 nM) for 48 h or with the MAO inhibitors pargyline (1 μ M) and moclobemide (1 μ M) (A and C) for 30 min prior to stimulation with IL-13 (2 nM) (A and C) for 48 h. A and C, native MAO-A enzyme activity was detected by MAO-GLO assay as described earlier. Data are represented as mean \pm S.D. ($n = 3$, $p < 0.005$). B and D, A549 and primary monocyte lysates (50 μ g/well) were incubated with Amplex Red reagent/HRP/p-tyramine working solution for 60 min before the fluorescence was measured. Data are represented as means \pm S.D.; ($n = 3$, $p < 0.005$). Data in all panels are from a representative of three independent experiments.

the specificity of 15-LO-mediated regulation of MAO-A gene expression in IL-13-activated monocytes.

Native MAO-A enzyme activity is also dependent on 15-LO in IL-13-activated A549 cells and in primary monocytes/macrophages

We further show that in addition to the direct involvement of 15-LO in regulating MAO-A expression in A549 cells and in alternatively activated monocytes/macrophages by IL-13, 15-LO also directly controls MAO-A enzymatic activity in IL-13-stimulated A549 cells and in monocytes/macrophages. To determine the role of 15-LO on IL-13-induced MAO-A activity in these cells, we adopted both MAO-GLO as well as Amplex Red monoamine oxidase assay. We transfected A549 cells and monocytes both with MAO-A and 15-LO antisenses along with their sense controls. In MAO-GLO assay we treated the cells with IL-13 and performed the chemiluminescence-based assay using the manufacturer's protocol. The results from our assay show that both MAO-A- and 15-LO-specific anti-

sense ODNs significantly attenuated MAO-A enzyme activity compared with IL-13-treated positive control, whereas their sense ODN controls show no effect on MAO-A activity in IL-13-activated A549 cells and in primary monocytes/macrophages (Fig. 6, A and C). In this assay we also included two inhibitors of MAO enzyme activity. One is the pan-MAO inhibitor pargyline, and the other is MAO-A-specific inhibitor moclobemide. Both these inhibitors substantially inhibited the MAO-A enzymatic activity compared with the IL-13-stimulated group (Fig. 6, A and C). These results thus confirmed the specificity of the assay and demonstrated the role of 15-LO in regulating MAO-A activity in IL-13-stimulated A549 cells as well as in primary monocytes. To reconfirm our observation by a second method, we did a similar experiment using the Amplex Red assay of MAO-A. Our results further confirm that both MAO-A and 15-LO antisenses markedly reduced IL-13-mediated H_2O_2 generation in the presence of *p*-tyramine in A549 cells and in monocytes/macrophages, whereas the sense ODN controls showed no effect (Fig. 6, B and D). These results

Regulation of MAO-A in IL-13-activated cells

unequivocally support that 15-LO directly regulates MAO-A enzymatic activity in A549 cells and in primary monocytes/macrophages in response to IL-13 stimulation.

IL-13-dependent expression of MAO-A in A549 and in primary monocytes requires the involvement of PPAR γ

As 15-LO products HPODE/HPETE are well-known PPAR γ ligands, we next explored the possibility that IL-13-induced MAO-A gene expression in human monocyte/macrophage and in A549 cells is mediated by coordinate induction of 15-LO and PPAR γ . Hence, we investigated the probable involvement of PPAR γ and the mechanistic details associated with 15-LO-mediated MAO-A expression in A549 as well as in primary human monocytes in response to IL-13 stimulation. Our results showed that the PPAR γ antagonist GW9662 significantly down-regulated the mRNA expression of MAO-A in IL-13-activated A549 cells (Fig. 7A). A similar effect of GW9662 was observed in primary monocytes where IL-13-induced MAO-A mRNA expression is also reduced substantially by the addition of GW9662 in a dose-dependent manner (Fig. 7C).

As we reported that the IL-13-activated MAO-A gene expression depends on 15-LO and 15-LO generates the PPAR γ ligand (13S)-HPODE and its stable form (13S)-HODE, we next investigated the effect of addition of these fatty acids on the restoration of MAO-A gene expression in those cells that are already treated with the 15-LO antisense (followed by incubation with IL-13) to establish a direct role of PPAR γ and its ligand in IL-13-induced MAO-A expression. We already provided evidence that IL-13 induction of MAO-A mRNA expression was significantly reduced by the pre-treatment with a selective 15-LO activity inhibitor PD146176 in monocytes in a dose-dependent manner (Fig. S6A). Here, we further confirmed this observation by the presence of 15-LO antisense ODN in A549 cells (Fig. 7A) and in primary monocytes (Fig. 7B). Addition of the 15-LO product (13S)-HPODE at the indicated doses restored MAO-A expression either in the presence of PPAR γ antagonist GW9662 (Fig. 7A) or 15-LO AS ODN almost completely in IL-13-activated A549 cells (Fig. 7A). A similar restoration effect of MAO-A expression by (13S)-HPODE was also observed in 15-LO AS-treated primary monocytes after IL-13 stimulation (Fig. 7B). (13S)-HODE demonstrated a similar effect where it counteracted the effect of 15-LO AS after IL-13 activation in primary monocytes (Fig. 7B). To check the specificity of this experiment, we treated primary monocytes with the MAO-A-specific antisense or control sense ODNs before IL-13 induction. Treatment of MAO-A-specific antisense significantly reduced the MAO-A mRNA expression level, whereas the sense control is without effect (Fig. 7B).

It was further shown that the PPAR γ ligand (13S)-HPODE successfully restored the effect of Stat6 decoy ODN on IL-13-stimulated mRNA expression of MAO-A in primary monocytes (Fig. 7C), confirming that the involvement of PPAR γ in regulation of IL-13-induced MAO-A expression is also Stat6-dependent. Furthermore, we demonstrate here that both (13S)-HPODE and (13S)-HODE profoundly up-regulated the expression of MAO-A mRNA in A549 cells (Fig. 7A) and in primary monocytes (Fig. 7C) even in the absence of IL-13. These results thus show that 15-LO-dependent regulation of MAO-A

expression in IL-13-activated cells is mediated by PPAR γ and that Stat6 might be involved in the PPAR γ -mediated regulation of MAO-A gene expression. In addition, PPAR γ is also involved in regulating MAO-A expression in A549 cells and in primary monocytes even in the absence of IL-13.

Stat6 directly interacts with PPAR γ in IL-13-activated A549 cells

We next focused on resolving the intricate mechanisms associated with PPAR γ -mediated MAO-A gene transcription in IL-13-stimulated cells. We first checked whether IL-13 treatment could enhance the expression level of PPAR γ . Our results showed that IL-13 could not induce the expression of PPAR γ protein, which was already present constitutively in A549 cells (Fig. 8A). Our previous experiment, related to the involvement of Stat6 in PPAR γ -mediated MAO-A gene expression, raised the possibility of interaction between these two transcription factors. Hence, we performed the co-immunoprecipitation (co-IP) experiment in A549 lung epithelial carcinoma cells to show that endogenously expressed PPAR γ and Stat6 physically interact with each other after IL-13 administration for 5 h (this interaction can be seen even after 1 h of IL-13 treatment, data not shown), and this association remains intact even after 5 days of IL-13 incubation (Fig. 8B) when 15-LO and MAO-A induction still persists in A549 cells (data not shown). As Stat6 is tyrosine-phosphorylated even after 5 h of IL-13 exposure (Fig. S1F), we next checked whether Stat6 in co-IPs is phosphorylated in response to IL-13 treatment (for 5 h) by probing the co-immunoprecipitated sample with p-Tyr-Stat6 antibody. Our results confirmed that Stat6 is in its tyrosine-phosphorylated (activated) form when it associates with PPAR γ (Fig. 8C). In continuation of our Stat6 decoy ODN experiment, which showed reduced expression of MAO-A mRNA (Fig. 7C), we further performed the co-IP experiment after transfecting the A549 cells with Stat6 decoy ODN along with the Stat6 scrambled ODN control to examine whether the Stat6 decoy ODN has any effect on IL-13-induced PPAR γ -Stat6 association. Our results demonstrate that in this competition experiment, endogenously present Stat6 interacts more with the Stat6 decoy ODNs thereby less and less endogenous Stat6 is available for interaction with PPAR γ (Fig. 8D), whereas Stat6 scrambled ODN has no effect on PPAR γ -Stat6 interaction. These results thus show that the interaction between Stat6 and PPAR γ is necessary for PPAR γ -mediated gene transcription in IL-13-activated cells.

Stat6 facilitates PPAR γ activation and PPAR γ -mediated MAO-A gene expression in response to IL-13 stimulation

We next investigated whether the interaction between Stat6 and PPAR γ is required for PPAR γ activation and PPAR γ -mediated MAO-A gene expression in IL-13-stimulated cells. We discovered that IL-13 induced PPAR γ activation (endogenous PPAR γ DNA binding with its consensus DNA-binding sequence) in A549 as well as in primary monocytes (Fig. 8, E and F). In the presence of Stat6 decoy ODN, when the association between PPAR γ and Stat6 is diminished, PPAR γ activation (DNA-binding activity) was also significantly reduced compared with the IL-13-treated control group in both A549 cells and in primary monocytes (Fig. 8, E and F), suggesting that

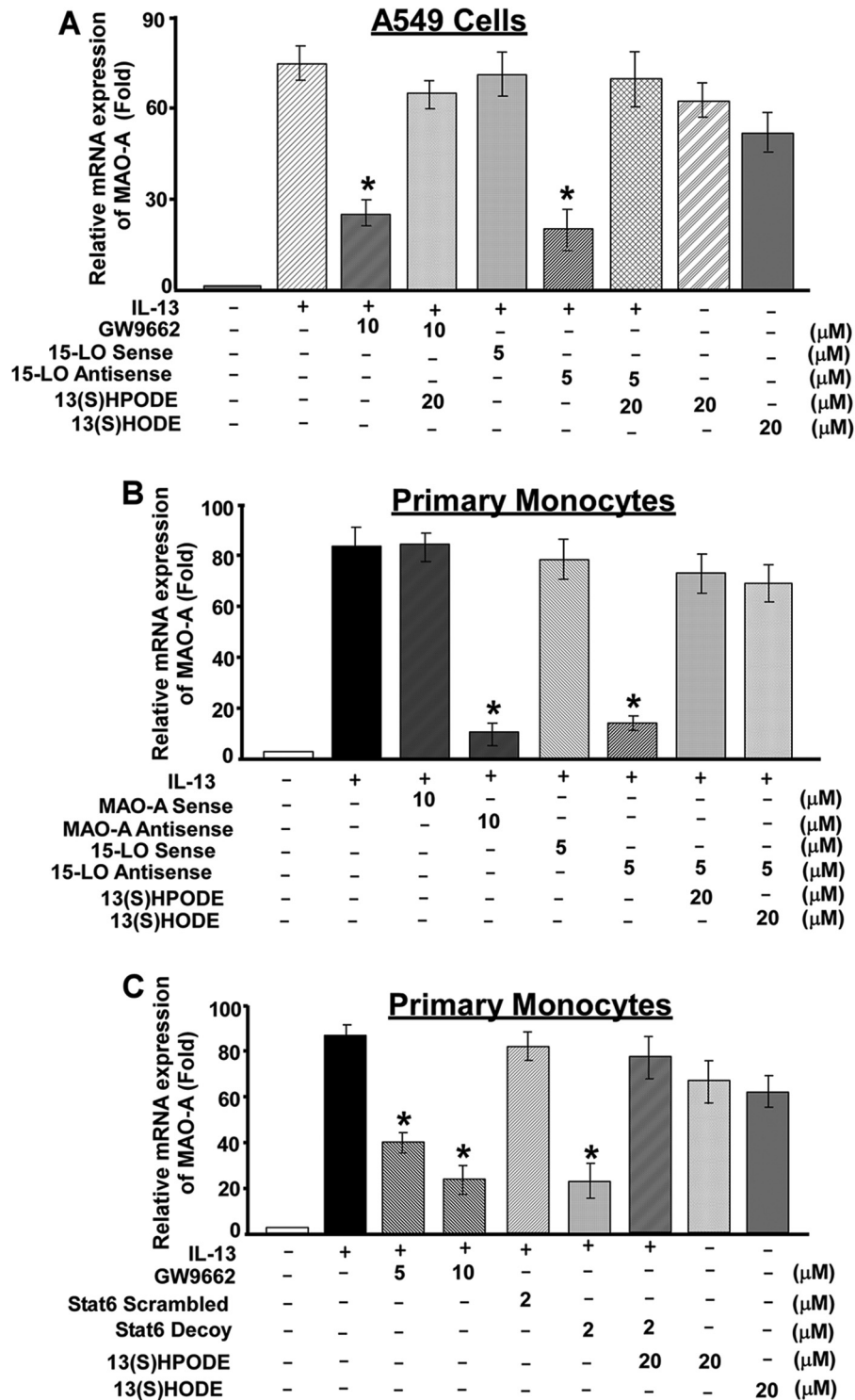


Figure 7. 15-LO inhibitor and antisense as well as PPAR γ antagonist block MAO-A expression in A549 cells and primary monocytes by IL-13, whereas (13S)-HPODE and (13S)-HODE counteract the effect of PPAR γ antagonist as well as 15-LO antisense. A549 cells and primary monocytes (5×10^6 /group) were either pretreated with 15-LO and MAO-A antisense (AS) or sense (S) ODNs (A and B) for 48 h or transfected with decoy or scrambled decoy ODNs to Stat6 (C) for 24 h followed by stimulation with IL-13 for 24 h (A–C). In some groups, (13S)-HPODE (20 μ M) and (13S)-HODE (20 μ M) were added either directly (for 24 h) (A and C) or after 24 h of IL-13 incubation (HPODE and HODE addition in AS-treated group or in decoy ODN-treated group for 24 h) as shown in A–C. A and C, A549 cells and monocytes were also pretreated with the PPAR γ antagonist GW9662 (at indicated doses) for 30 min followed by stimulation with IL-13 for 24 h. In one group in A, (13S)-HPODE was added in GW9662-pretreated group after IL-13 incubation for 24 h and exposed for another 24 h. A–C, total cellular RNA extracts were prepared and subjected to quantitative real-time PCR analysis. After normalization with GAPDH amplification, the fold induction of MAO-A mRNA expression for different groups was plotted. Values are mean \pm S.E. of three separate experiments. *, $p < 0.05$ compared with the IL-13-treated group.

Regulation of MAO-A in IL-13-activated cells

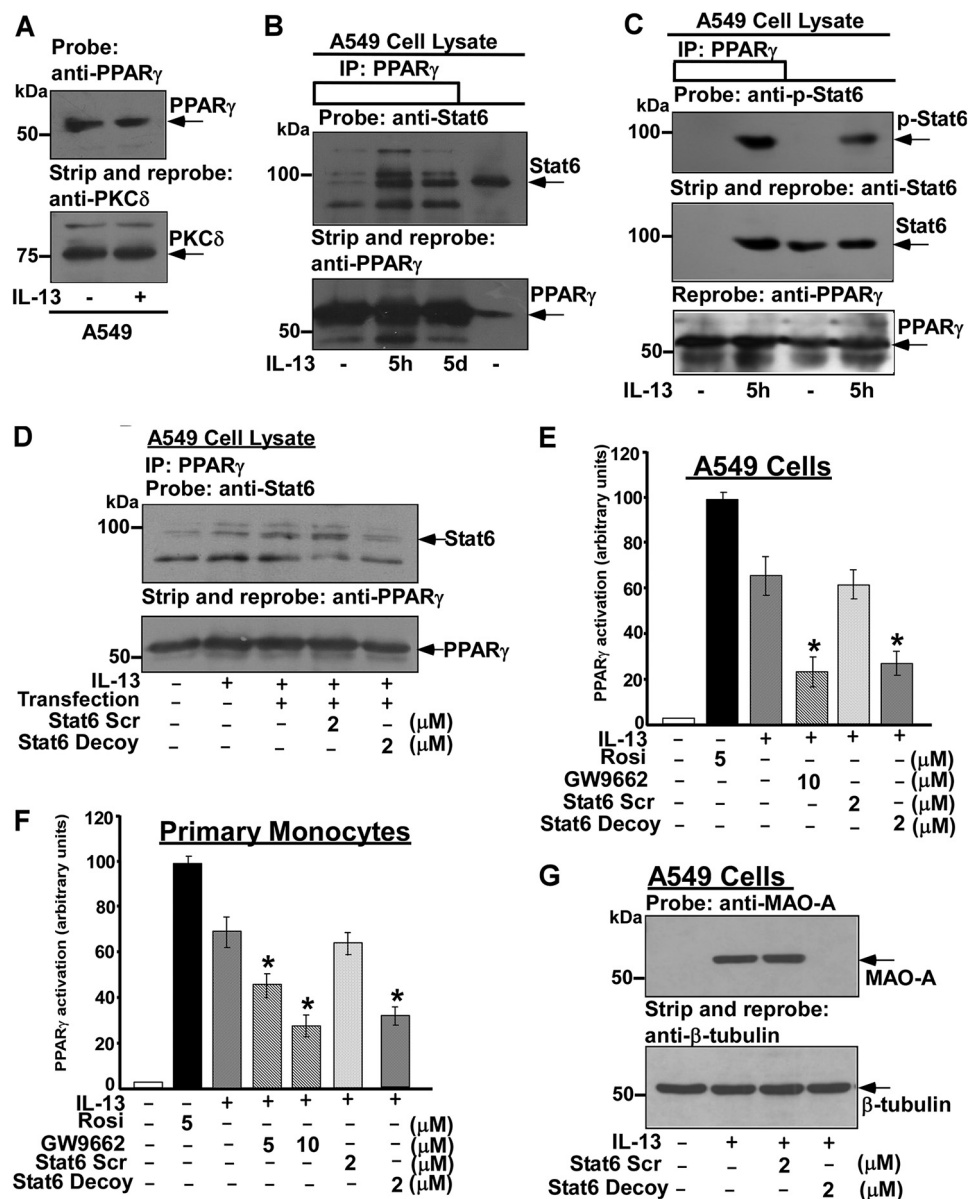


Figure 8. IL-13-induced PPAR γ activation and MAO-A gene expression depends on Stat6. A549 cells (5×10^6 /group) were either left untreated or treated with IL-13 for 5 h. Cell lysates (total) were assessed for PPAR γ protein expression level by Western blot analysis (upper panel of A). The same blot was then stripped and reprobbed with PKC δ antibody to show equal loading (lower panel of A). B and C, physical interaction between Stat6 and PPAR γ was investigated by immunoprecipitation (IP) assay. A549 cells (5×10^6 /group) were either left untreated or treated with IL-13 for 5 h (B and C) and 5 days (B). Cell lysates (total) were immunoprecipitated with PPAR γ antibody (B and C) followed by Western blot analysis using Stat6 (upper panel of B and middle panel of C) and phospho-Tyr-Stat6 (upper panel of C) antibodies. Untreated (B and C) and IL-13-treated (C) A549 cell lysates (total) were run alongside as controls. The blots were then stripped and reprobbed with PPAR γ antibody to assess equal loading of immunoprecipitated samples (lower panels of B and C). D, effect of Stat6 decoy ODN on Stat6 and PPAR γ association was studied by transfection of Stat6 scrambled and decoy ODNs into A549 cells (5×10^6 /group) using PEI transfection reagent. After 48 h post-transfection, IL-13 incubation was carried out for another 5 h. Cell lysates (total) were immunoprecipitated using PPAR γ antibody and subjected to immunoblot analysis using Stat6 antibody (upper panel of D). The same blot was then stripped and reprobbed with PPAR γ antibody to assess equal loading (lower panel of D). E–G, A549 cells and monocytes (5×10^6 /group) were either transfected with or without decoy or scrambled decoy ODNs to Stat6 (E, F, and G) for 24 h followed by stimulation with IL-13 for 1 h (E and F) or for 48 h (G). Monocytes were also treated with either rosiglitazone (Rosi) or IL-13 (2 nM) for 1 h or pretreated with indicated doses of PPAR γ antagonist GW9662 for 30 min followed by stimulation with IL-13 for 1 h (E and F). E and F, nuclear extracts were prepared, and 10 μ g of nuclear proteins were used to perform an immunodetection of activated PPAR γ using a TransAM™ kit. The data are represented as relative arbitrary units with rosiglitazone treatment set at 100. Data are represented as means \pm S.E. of three independent experiments giving similar results. Significant differences were determined by comparing each group to the IL-13-treated A549 and monocytes as controls (*, $p < 0.01$). G, A549 cell lysates (postnuclear) were separated by SDS-PAGE and immunoblotted with MAO-A (upper panel of G) antibody. The same blot was then stripped and reprobbed with β -tubulin antibody (lower panel of G) to assess equal loading. Data in G are from a representative of three independent experiments showing similar results.

PPAR γ DNA-binding activity depends on its interaction with Stat6. In contrast, Stat6-scrambled ODN showed no inhibition. As control for monitoring PPAR γ DNA-binding activity, we tested whether the PPAR γ ligand rosiglitazone could induce PPAR γ activation and whether GW9662, the PPAR γ antago-

nist, could inhibit the IL-13-induced PPAR γ activation. Our results further demonstrate that PPAR γ activation is enormously induced in the presence of rosiglitazone, whereas GW9662 significantly blocked the IL-13-induced PPAR γ DNA-binding activity (Fig. 8, E and F). To determine whether

Stat6–PPAR γ interaction followed by PPAR γ activation is critical for *MAO-A* gene expression in IL-13-activated cells, we transfected A549 cells with both Stat6 decoy ODN or Stat6 scrambled ODN. Our data reveal that in presence of Stat6 decoy ODN, when the interaction between Stat6 and PPAR γ is significantly diminished and PPAR γ DNA-binding activity is markedly reduced, the IL-13-induced MAO-A protein and mRNA expression is almost completely blocked compared with the IL-13-treated positive control (Figs. 8G and 7C). In contrast, Stat6 scrambled ODN had no inhibitory effect. These results thus suggest that Stat6 acts as a facilitator of PPAR γ activation and PPAR γ -mediated regulation of *MAO-A* gene expression in IL-13-activated cells.

IL-13-dependent MAO-A expression and activity are regulated by PPAR γ but do not require the involvement of Stat6 and 15-LO in U937 monocytic cells

Although myeloid cell lines like U937 promonocytic cells are highly proliferative and malignant cells have numerous differences from monocytes/macrophages, they are often used as an experimental model for primary human monocytes. U937 cells also have some technical advantages over human primary monocytes or macrophages. For instance, their genetic background is homogeneous, which minimizes the degree of variability in the cell phenotype. Hence, U937 cells are widely used as a model monocytic system in the laboratory for routine cell biology experiments. Considering all these aspects, it is really important to know whether the same control mechanism is valid for IL-13-activated *MAO-A* gene expression in U937 promonocytic cells, which exist in primary monocytes and in A549 cells.

Based on our preliminary data, which showed that 15-LO is neither expressed, nor induced by IL-13 in U937 cells (Fig. 1I), we predicted that 15-LO might not be involved in regulating MAO-A expression and activity in U937 cells in response to IL-13 stimulation. To conclusively determine the role of both PPAR γ and 15-LO, we carried out experiments using the PPAR γ antagonist GW9662 and 15-LO antisense ODN to check the expression of MAO-A protein and mRNA in U937 cells after IL-13 stimulation. Although pretreatment of U937 cells with the PPAR γ antagonist GW9662 abrogated IL-13-induced MAO-A protein and mRNA expression, 15-LO antisense and Stat6 decoy ODN treatment showed no effect (data not shown). We further used PPAR γ ligand rosiglitazone and (13S)-HPODE (15-LO product) to analyze whether they can independently induce MAO-A expression in U937 cells. Our results showed that both of them substantially enhanced the level of MAO-A mRNA expression independent of IL-13 induction (data not shown).

Next, we checked the role of PPAR γ , Stat6, and 15-LO on MAO-A enzymatic activity by performing the MAO-GLO assay in U937 cells after transfecting the cells with decoy and antisense ODNs followed by IL-13 stimulation. Our results showed that Stat6 decoy ODN and 15-LO-specific antisense ODN had no inhibitory effect on MAO-A enzyme activity. In contrast, pretreatment of U937 cells with GW9662 showed substantial inhibition on IL-13-induced MAO-A enzyme activity (data not shown). From these results, we can conclude

that IL-13-dependent expression and activity of MAO-A in U937 cells require PPAR γ activation but are independent of Stat6 and 15-LO expression/activity.

IL-13-stimulated migration of A549 tumor cells and primary human monocytes is mediated by MAO-A and requires both PPAR γ and 15-LO activity

As we already demonstrated that IL-13-induced *MAO-A* gene expression and activity in A549 lung epithelial carcinoma cells and in primary monocytes are modulated by both PPAR γ and 15-LO, we next wanted to investigate whether MAO-A-mediated cellular function is also governed by these two critical regulators. To evaluate the role of PPAR γ and 15-LO on IL-13-activated A549 cell migration mediated by MAO-A, we utilized an *in vitro* transwell migration assay using the MAO-A activity inhibitor moclobemide along with the 15-LO inhibitor PD146176 and PPAR γ antagonist GW9662. In Fig. 9, A and B, we first compared IL-13-induced A549 cell migration data with metformin (8 mM)-treated A549 cells as positive control (44). Next, we represented data in Fig. 9C, which suggest that IL-13 treatment resulted in a significant enhancement of A549 cell migration compared with the untreated control. In the presence of moclobemide, IL-13-induced A549 cell migration is reduced substantially, whereas moclobemide alone in absence of IL-13 showed no change compared with the unstimulated control (Fig. 9C), thereby suggesting a plausible role of MAO-A in A549 tumor cell migration *in vitro*. Fig. 9D represents microscopic images showing a significantly less number of cells migrating following moclobemide treatment as compared with IL-13-stimulated A549 cells.

Significant reduction of migration was also observed in IL-13-activated A549 cells after treatment with the 15-LO activity inhibitor PD146176 and PPAR γ antagonist GW9662 in a dose-dependent manner (Fig. 9, E and G) compared with IL-13-stimulated positive control. Corresponding microscopic images presented in Fig. 9, F and H, also showed that significantly fewer A549 cells migrated after PD146176 and GW9662 treatment with the indicated doses mentioned here as compared with IL-13-activated A549 cells. We further checked whether the chemical inhibitors that are used for the experiments presented in Fig. 9 have any effect on cell viability at the indicated doses. Our MTT assay data shown in Fig. S7, A–C, suggest that the doses at which moclobemide, PD146176, and GW9662 substantially reduced the migration of IL-13-activated A549 cells have no inhibitory effect on the viability of A549 cells for the stipulated time period. We also examined whether inhibition of MAO-A activity by the specific inhibitor moclobemide has any significant effect on A549 cell viability and proliferation. Our additional experiments (trypan blue exclusion assay and MTT assay) provide evidence that there is no effect of the MAO-A inhibitor moclobemide (at 10 μ M dose) on the A549 cell number as compared with IL-13-treated control (Fig. S7, D and E). These experiments thus act as control for the potential effects of cell number on the migration observation as represented in Fig. 9C.

To establish the similar regulatory mechanisms for the migration of IL-13-activated primary monocytes, we followed the chemotaxis assay using a microchamber technique. Here,

Regulation of MAO-A in IL-13-activated cells

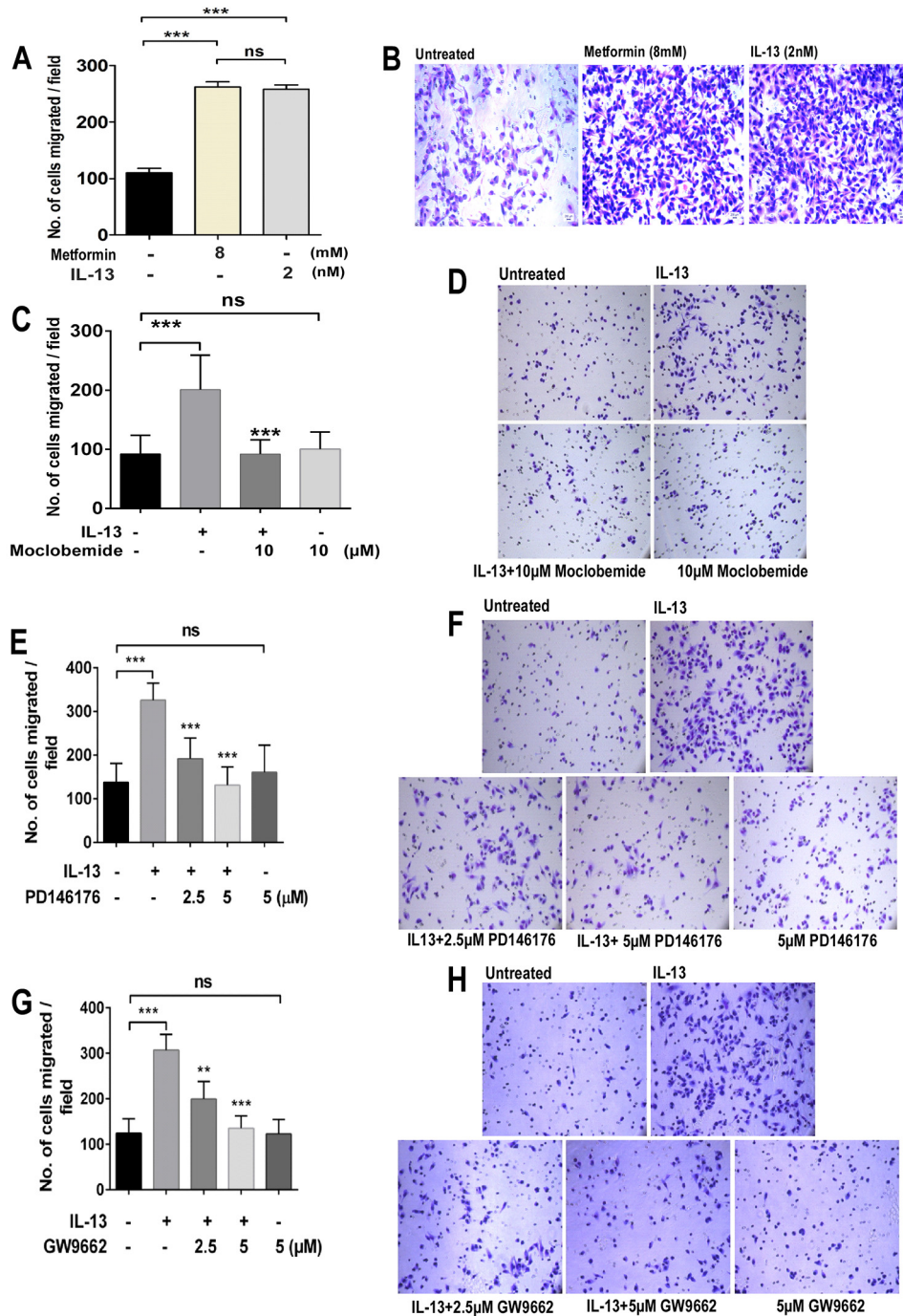


Figure 9. Reduction of MAO-A, 15-LO, and PPAR γ activity resulted in significant inhibition of IL-13-induced A549 cell migration. A549 cells were either directly treated with IL-13 (2 nM) for 96 h (A) or pretreated with MAO-A inhibitor moclobemide, 15-LO-specific inhibitor PD146176, as well as PPAR γ antagonist GW9662 for 30 min followed by IL-13 treatment for 96 h (C, E, and G). A, metformin (8 mM) treatment of A549 cells (for 96 h) was considered as a positive control. A, C, E, and G, *in vitro* transwell migration assay was performed. Briefly, 5 h after seeding 1.5×10^5 cells (in presence of serum free DMEM) in the upper chamber of 12-well inserts, cells that migrated through the membrane of the transwell toward DMEM with 15% FBS were fixed and stained with Giemsa. Migrated cells from six random fields were counted under microscope. Data were analyzed by one-way ANOVA (Dunn test). A, C, E, and G, data are represented as mean \pm S.D. ($n = 3$, ***, $p < 0.001$; **, $p < 0.01$). Data in all panels are from a representative of three independent experiments showing similar results. Representative microscopic images of migrated A549 cells in different inhibitor treated groups in presence and absence of IL-13 stimulation were also shown in B, D, F, and H, respectively.

we also compared our migration data in primary human monocytes (after IL-13 incubation for 48 h) (Fig. 10A) with monocyte migration in response to MCP-1 (50 ng/ml) for 90 min (45–47). We then initiated our studies by using both the pharmacological inhibitor (moclobemide) as well as specific antisense ODN against MAO-A. Our results suggest the involvement of

MAO-A in regulating the migration of IL-13-activated primary monocytes as both moclobemide (dose-dependently) and MAO-A antisense showed significant reduction of migration of IL-13-stimulated monocytes, whereas MAO-A sense ODN control is without effect (Fig. 10B). The role of 15-LO and PPAR γ in MAO-A-mediated monocyte migration

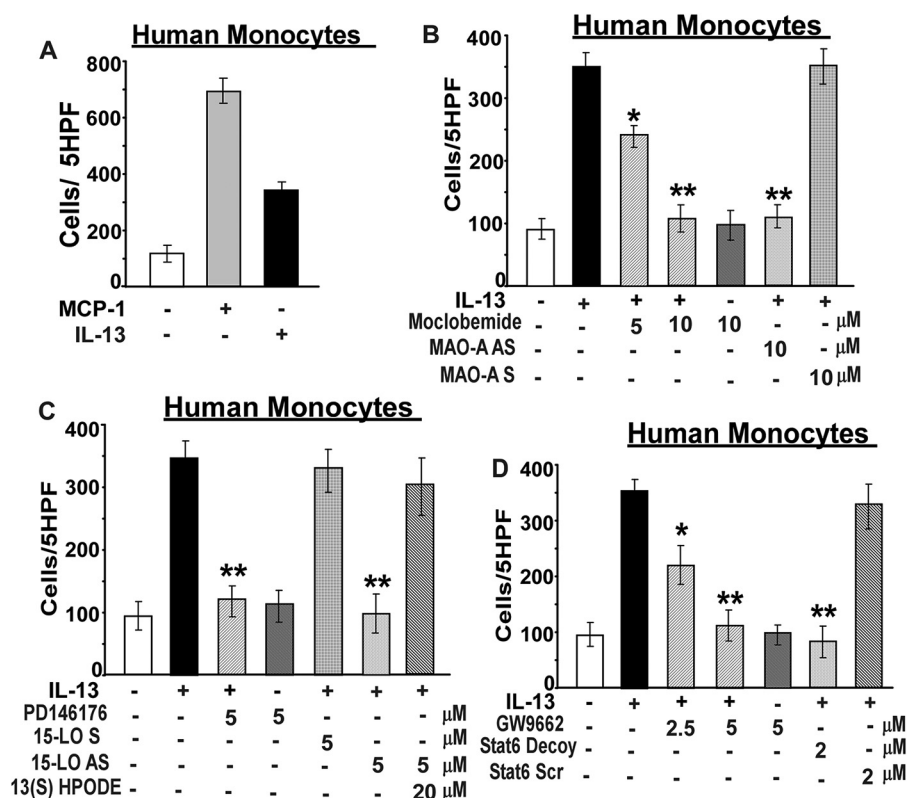


Figure 10. MAO-A and PPAR γ -mediated migration of IL-13-activated primary monocytes depend on 15-LO expression/activity. Primary human monocytes (5×10^6 /group) were either directly treated with IL-13 (2 nM) for 48 h (A) or pre-treated with sense and antisense ODNs to MAO-A (B) and 15-LO (C), decoy and scrambled decoy ODNs to Stat6 (D) or with the MAO-A and 15-LO inhibitors, moclobemide (B) and PD146176 (C) at indicated doses for 30 min prior to stimulation with IL-13 (2 nM) for 48 h. Cells were also pretreated with indicated doses of PPAR γ antagonist GW9662 for 30 min followed by IL-13 stimulation for 48 h (D). In some groups, (13S)-HPODE was added after 48 h of IL-13 incubation (HPODE addition in 15-LO AS-treated group for 24 h, C). A, monocyte migration in response to MCP-1 (50 ng/ml) for 90 min was considered as a positive control. A–D, monocyte chemotaxis across a polycarbonate filter in response to 15% FBS in DMEM was then measured as described earlier. All experiments were performed in triplicate. The results are expressed as the mean number of migrated monocytes in five high-power fields \pm S.D. ($\times 400$ light microscope) and are representative of three similar experiments. *, $p < 0.05$; **, $p < 0.005$ (compared with the IL-13-treated group) from one-way ANOVA. Data in all panels are from a representative of three independent experiments showing similar results.

was further assessed by using both 15-LO activity inhibitor PD146176 as well as 15-LO-specific antisense ODN and PPAR γ antagonist GW9662. We demonstrated that PD146176 and 15-LO antisense ODN both markedly abrogated the ability of IL-13-activated monocyte migration, whereas the 15-LO sense ODN control had no effect (Fig. 10C). We further showed that the PPAR γ ligand (13S)-HPODE could restore the effect of 15-LO antisense ODN on monocyte migration (Fig. 10C). In Fig. 10D, we provided evidence that PPAR γ antagonist GW9662 significantly inhibited the IL-13-stimulated monocyte migration in a dose-dependent way. Furthermore, our results reveal that Stat6 decoy ODN also blocked the migration of primary monocytes at a substantial level after IL-13 stimulation, whereas the Stat6 scrambled ODN showed no effect (Fig. 10D). Altogether, these results confirm the requirement of PPAR γ and 15-LO activity/expression in MAO-A-mediated migration of IL-13-activated primary monocytes.

MAO-A-mediated ROS generation in presence of tyramine requires both PPAR γ and 15-LO activity/expression in IL-13-activated A549 cells and in monocytes

Previously, we reported that generation of intracellular ROS during the oxidation of biogenic amine-like tyramine by MAO-A in alternatively activated monocytes/macrophages by

IL-13 (1). In this report, we continued this study and investigated the mechanistic details of the MAO-A-mediated ROS generation in IL-13-activated monocytes and other cells in the presence of tyramine. As a control, we first showed that moclobemide (a specific inhibitor for MAO-A) strongly inhibited the tyramine induction of intracellular ROS generation in IL-13-activated A549 cells and in primary monocytes (Fig. 11, A and B). Furthermore, the involvement of both PPAR γ as well as 15-LO in controlling MAO-A-mediated ROS generation was also examined in A549 cells and in primary monocytes after IL-13 induction. Our results produced evidence that the 15-LO activity inhibitor PD146176 and antisense ODN against 15-LO both significantly blocked the tyramine-induced enhancement of intracellular ROS generation in IL-13-stimulated A549 and in primary monocytes (Fig. 11, A and B), whereas the sense ODN control for 15-LO had no effect. Moreover, (13S)-HPODE, the 15-LO product that also acts as a ligand of PPAR γ , rescued back the effect of 15-LO antisense ODN on MAO-A-mediated ROS generation in IL-13-stimulated cells (Fig. 11, A and B). The PPAR γ antagonist GW9662 also executed a strong reduction of ROS generation during tyramine oxidation of MAO-A in IL-13-activated A549 cells and in monocytes/macrophages (Fig. 11, A and B). In the presence of Stat6 decoy

Regulation of MAO-A in IL-13-activated cells

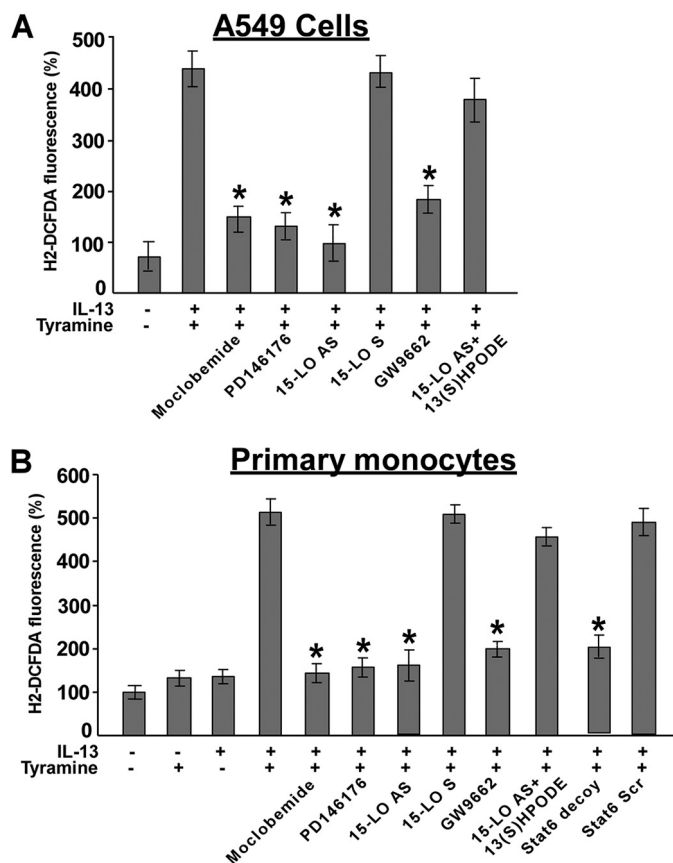


Figure 11. Tyramine-induced ROS generation is regulated by 15-LO in IL-13-activated A549 cells and in human monocytes/macrophages. A549 cells and primary human monocytes (5×10^6 /group) were pre-treated with sense and antisense ODNs to 15-LO (A and B), decoy, and scrambled decoy ODNs to Stat6 (B) or with the MAO-A and 15-LO inhibitors, moclobemide (1 μ M) and PD146176 (5 μ M) (A and B) for 30 min prior to stimulation with IL-13 (2 nM) for 24 h. All type of cells were also pretreated with 5 μ M GW9662 for 30 min followed by IL-13 stimulation for 24 h (A and B). In some groups in A and B, (13S)-HPODE (20 μ M) was added after 24 h of IL-13 incubation (HPODE addition in AS-treated group for 24 h). A and B, cells were stimulated by tyramine (5 μ M) for 30 min and then incubated with the fluorescent probe H₂DCFDA (5 μ M) for another 30 min before the fluorescence was measured. Data in A and B are expressed as percentage of unstimulated controls and represented as means \pm S.D.; ($n = 3$, $p < 0.005$). Data are from a representative of three independent experiments.

ODN, again the function of MAO-A is controlled as evidenced by the significant attenuation of ROS generation level in IL-13-activated monocytes/macrophages, whereas Stat6-scrambled ODN had no effect (Fig. 11B).

Altogether, these data strongly suggest that IL-13 signal transduction uses a distinct 15-LO and PPAR γ -dependent mechanism that is regulated by Stat6 in A549 cells and in primary monocytes/macrophages to control the IL-13-driven function of MAO-A in tyramine-induced ROS generation.

Discussion

In this study, we demonstrated that during IL-13 stimulation 15-lipoxygenase and MAO-A are the two strongly up-regulated genes that are co-induced in primary monocytes/macrophages, A549 lung carcinoma cells, and in normal human bronchial epithelial (NHBE) cells. In contrast, MAO-A is induced in the human promyelomonocytic cell line, U937, by IL-13 stimulation independent of 15-lipoxygenase induction. Considering

the role of MAO-A in the resolution of inflammation and its other pathophysiological implications (48), it is an extremely important requirement to carry out a detailed investigation to understand the regulatory mechanisms associated with the expression and function of MAO-A during IL-13 activation of primary monocyte/macrophages, A549 lung carcinoma cells, and in U937 promonocytic cells, which is also the primary focus of this study. The outcome of this study, however, shows that IL-13 induction of MAO-A has a major contribution in the resolution of inflammation (in monocyte/macrophage system) and in enhancement of the metastatic potential of cancer cells (in A549 lung cancer).

Our investigations further suggest that in many other cancer cells like in H1299 NSCLC (Fig. 2, A and B), in HCT116 colorectal cancer cells, or in PC3 prostate cancer cells (data not shown), MAO-A is constitutively overexpressed, and IL-13 is not involved in the further induction of MAO-A in these cells. The discrepancies between the observations in H1299, NSCLC, HCT116, and PC3 cells on the one hand and in A549 and NHBE cells on the other hand can be explained by the fact that in H1299, HCT116, or in PC3 cells, the relative expression level of the decoy receptor (IL-13R α 2) is probably very high compared with the IL-13R α 1 component that may affect the normal IL-13 signaling. In contrast, in A549 or in NHBE cells, the case may be just reverse which promotes the normal IL-13 signaling leading to the induction of both 15-LO and MAO-A genes in a concordant manner. The new observations in NHBE cells (Fig. 2, C–F) also show that the signaling module to be investigated is not restricted only in primary monocytes/macrophages and A549 lung carcinoma cells, and they bring more impact of our findings in other pathophysiological processes like asthma.

Our findings regarding the co-induction of MAO-A and 15-LO in IL-13-activated peripheral blood monocytes and in A549 cells suggest a common regulatory pathway for the expression of these two genes. Previously, we provided evidence for the involvement of the same Jaks and Stats in regulating MAO-A gene expression that are required for 15-LO gene expression in IL-13-activated monocytes (1). Here, we further demonstrate that Egr1 and CREB, the two crucial transcription factors that control 15-LO gene expression (15), are also involved in regulating MAO-A gene expression. Furthermore, based on the *in silico* promoter analysis studies, we speculated the existence of Stats (Stat1, Stat3, and Stat6), Egr-1, and CREB-binding sites located in the promoter of the 15-LO gene and validated our predictions by performing experiments that showed the direct binding of Stats (Stat1, Stat3, and Stat6), Egr1, and CREB transcription factors to their cognate DNA-binding sites in the context of flanking sequences present in the 15-LO promoter (this study and see Ref. 15). All these observations led us to speculate that the promoter of the MAO-A gene may also contain the cognate sequences for the binding of the same transcription factors. Although our *in silico* structural promoter analysis failed to detect any Stat, Egr-1, or CREB-responsive sequences in the 5'-flanking region of MAO-A gene promoter (this study), the discrepancies between these observations can be explained by the fact that these transcription factors may not be directly involved in regulating MAO-A gene expression. This hypothesis is directly supported by the obser-

vation in this study that 15-LO antisense oligonucleotide transfection significantly inhibits IL-13-induced MAO-A gene expression in primary human monocytes and in A549 cells. We provide evidence for the first time that in case of primary monocytes/macrophages, the MAO-A gene expression and activity are directly regulated by 15-LO, which is specifically co-induced during the alternative activation of monocytes/macrophages by IL-13 (no induction of MAO-A or 15-LO during conventional activation by LPS or IFN γ), and has a considerable impact in the resolution of inflammation.

We explored the regulatory mechanisms that control the expression/activity and function of MAO-A, a crucial marker of alternative activation of primary monocytes. Our investigation reveals the existence of several regulatory pathways that are all PPAR γ -dependent but either 15-LO-dependent or -independent during IL-13 activation. In primary monocyte/macrophages and in A549 cells, 15-LO is co-induced with MAO-A by IL-13 stimulation due to the presence of an unmethylated 15-LO promoter in these cellular systems. In contrast, the 15-LO promoter is exclusively methylated in U937 cells and thereby incapable of expressing the 15-LO gene after IL-13 activation (49). Hence, the IL-13-induced MAO-A gene expression/function is independent of 15-LO in U937 cells.

PPAR γ is a lipid-activated transcription factor regulating cellular lipid metabolism and inflammation (50–53). Requirement of PPAR γ activity for alternative activation of macrophages is already reported (54, 55). Although alternative activation of macrophages by IL-4/IL-13 is linked with PPAR γ -mediated transcriptional regulation, the detailed mechanism of this process has yet to be explored. Moreover, it is also documented that the IL-4–Stat6–PPAR γ signaling axis is crucial for the differentiation of monocytes into alternatively activated macrophages and for innate immune responses (53, 56). Further studies demonstrated PPAR γ as a downstream effector of IL-4 signaling rather than a direct regulator of alternative activation of the monocyte/macrophage system (53, 56). During induction of 15-LO gene expression, 15-LO metabolites 15-HPETE/13-HPODE can act as potential ligands of PPAR γ , which control the PPAR γ -dependent gene expression. Moreover, our results in this study further suggest that Stat6, by interacting with PPAR γ , promotes PPAR γ 's DNA binding and finally facilitates the PPAR γ -mediated gene expression in IL-13-activated cells. The cross-talk between the two transcription factors (Stat6 and PPAR γ) to orchestrate the gene expression during IL-13 activation is not unprecedented and is previously reported between other transcription factors (57, 58), but the molecular details of this cross-talk remain to be determined and definitely need further study and clarification. Thus IL-13–Stat6–15-LO–PPAR γ axis may have considerable effect for monocyte/macrophage physiology and function during alternative activation and also on the resolution of inflammation.

Although the promyelomonocytic cell U937 is considered as the experimental model system for monocytes and is extensively used to carry out many *in vitro* experiments due to the stability, consistency, and reproducibility of the system, the promonocytic U937 cells cannot be considered as an appropriate model in the context of a real life situation. Based on the

differential regulation of IL-13-induced MAO-A expression and function between mature monocytes/macrophages and U937 promonocytes, primary monocytes represent the correct model system for the analysis of IL-13 activation of monocytes/macrophages.

Mature monocytes migrate toward sites of inflammation and infection where they differentiate into inflammatory macrophages or into dendritic cells. Monocyte migration into sites of inflammation is a crucial event for the pathogenesis of inflammatory and degenerative diseases. The mechanisms that control monocyte/macrophage trafficking under infectious and inflammatory conditions have not been fully elucidated. Our data presented in this study clearly show that MAO-A is a critical regulator of monocyte migration in IL-13-stimulated cells. This is the first report that provides strong evidence about the role of MAO-A in monocyte/macrophage chemotaxis. In addition, our data also establish the fact that in primary monocytes 15-LO–PPAR γ –MAO-A signaling axis is involved in regulating monocyte migration after IL-13 stimulation.

In cancer cells, migration and invasion are the initial steps that control metastasis, which is a predominant cause of cancer-related death. Recent reports reveal that MAO-A is involved in promoting prostate cancer progression by inducing epithelial to mesenchymal transition (EMT), which ultimately causes elevation of ROS, thus enhancing the ability of migration and invasion of these cells (39, 59). MAO-A enzymatic activity is shown to be the main cause of MAO-A-driven ROS generation in cancer cells, which acts as the critical regulator of MAO-A-mediated functions like migration, invasion, and proliferation (39, 59, 60). A recent report also suggests that IL-13 induces EMT phenotype in colorectal cancer cells by promoting migration and invasion of these cells via Stat6 activation (61). In an attempt to find out whether IL-13-induced MAO-A is involved in enhancing the aggressiveness of different types of cancer cells, we exposed different cancer cells to IL-13. We found that in many cases MAO-A is already constitutively present in these cells (not induced by IL-13 incubation) and promoting migration and invasion of these cells.⁵ A549 lung carcinoma cell is the unique cell type among the cancer cells where IL-13 induces MAO-A gene expression that causes increased migration and invasion (data not shown) and thereby enhances the metastatic potential of the lung cancer cells. Hence, these data in general propose that MAO-A is an important mediator of cancer metastasis. Our study also demonstrates for the first time that reactive oxygen species (ROS) are generated by MAO-A in IL-13-activated A549 lung epithelial carcinoma cells. As the MAO-A-mediated ROS generation is believed to have significant influence on A549 cell migration and cellular proliferation, we are interested in exploring the mechanistic details of this process in IL-13-activated A549 lung carcinoma cells. Furthermore, targeting MAO-A and disrupting its downstream signaling pathways may provide a promising therapeutic intervention in the pathogenesis of lung cancer.

In summary, we have uncovered the underlying mechanisms associated with MAO-A expression, activity, and function in

⁵ S. Dhabal, P. Biswas, and A. Bhattacharjee, unpublished observations.

Regulation of MAO-A in IL-13-activated cells

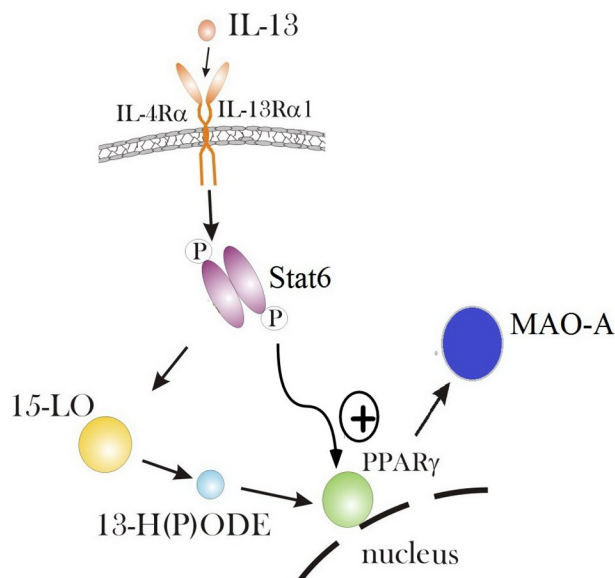


Figure 12. Schematic diagram showing the proposed mechanism of IL-13-induced MAO-A expression in primary human monocytes and A549 lung epithelial cancer cells.

IL-13-activated cells. Our results show the existence of IL-13-dependent and 15-LO-dependent regulation of MAO-A expression/activity in both primary human monocytes and in A549 lung epithelial carcinoma cells and clearly show the presence of an IL-13 > STAT6 > 15-LO > PPAR γ > MAO-A signaling cascade (Fig. 12), which ultimately governs the function of MAO-A, a critical enzyme involved in the resolution of inflammation and in the progression of cancer. In contrast, we provide evidence that IL-13-dependent but 15-LO-independent regulation of MAO-A expression/activity is operating in U937 monocytic cells. In the first case, endogenously produced 15-LO metabolite ((13S)-HPODE) can act as a ligand of PPAR γ and control the PPAR γ -mediated gene transcription. In the second case, IL-13 stimulation can lead to activation of PPAR γ by other ligands (other than (13S)-HPODE) and facilitate MAO-A gene transcription. In the absence of IL-13, exogenously added (13S)-HPODE can activate PPAR γ in all these cell types and further induce MAO-A gene expression/activity and function. We further demonstrate the inductive and cooperative relationship between Stat6 and PPAR γ in IL-13-dependent regulation of MAO-A expression/activity and function in both monocytes and A549 cells where Stat6 interacts with PPAR γ and acts as a positive regulator of PPAR γ -mediated gene transcription (Fig. 12). The salient features of our study are the result of MAO-A expression/activity being directly involved in the migration and tyramine-induced ROS generation in primary monocytes and A549 lung cancer cells. These studies have major implications for understanding the mechanism and function of alternatively activated monocytes/macrophages by IL-13 and add novel insights into the pathogenesis and potential treatment of different inflammatory diseases. Our results further indicate the probable contribution of MAO-A in lung cancer metastasis and suggest the potential of MAO-A as a therapeutic target in lung cancer.

Experimental procedures

Reagents

Recombinant human IL-13 and IFN- γ were purchased from BIOSOURCE and Invitrogen. The 15-LO standard and the rabbit reticulocyte 15-LO antibody, cross-reacting with human 15-LO, were raised in sheep and obtained as a gift from Dr. Joseph Cornicelli (Molecular Imaging). The other primary antibodies used in this study were as follows: MAO-A, PKC δ , PPAR γ , and β -tubulin from Santa Cruz Biotechnology (Santa Cruz, CA). Antibody to Stat6 was purchased from Pharmingen. Anti-phosphotyrosine-Stat6 (pTyr-641-Stat6) antibody was purchased from Cell Signaling Technology (Beverly, MA). ChemoTx Disposable Chemotaxis System (catalog no. 106-5) was purchased from Neuro Probe, Inc. (Gaithersburg, MD), and Hema 3 stain set (catalog no. 122-911) was from ThermoFisher Scientific (Pittsburgh, PA). The ROS-sensitive fluorescent probe 6-carboxy-2',7'-dichlorodihydrofluorescein diacetate, diacetoxyethyl ester (H₂DCFDA), was from Life Technologies, Inc. Amplex Red monoamine oxidase assay kit (catalog no. A12214) was from Molecular Probes (Invitrogen). MAO-GLO™ assay kit (catalog no. V1401) and MAO-A enzyme (human recombinant enzyme expressed in Yeast, catalog no. V1452) were purchased from Promega (Madison, WI). Polyethyleneimine (PEI) transfection reagent was also obtained as a kind gift from Dr. Mahadeb Pal, Bose Institute, India. LPS, Tyramine and pharmacological inhibitors such as pargyline (a pan-MAO inhibitor) and moclobemide (specific inhibitor for MAO-A) were purchased from Sigma. Rosiglitazone, GW9662, PD146176, (13S)-HPODE, and (13S)-HODE were from Cayman Chemical (Ann Arbor, MI). The inhibitors were stored either at room temperature or at -20 °C as concentrated stock solutions (either in water or DMSO) according to the manufacturer's instructions.

Ethics statement

All studies involving human subjects were approved by the Institutional Ethical Committee For Human Research, National Institute Of Technology, Durgapur, West Bengal, India. These studies abide by the Declaration of Helsinki principles.

Cell culture

A549 (human lung adenocarcinoma), H1299 (nonsmall cell lung cancer cell), and U937 (leukemic monocytic lymphoma) cells were procured from the central cell repository of the National Center for Cell Science (NCCS), Pune, India. The A549 and H1299 lung cancer cell lines were cultured in complete DMEM supplemented with 4.5 mg/ml glucose and other ingredients containing 10% FBS, 1 mM sodium pyruvate, 2 mM L-glutamine, nonessential amino acids, 100 units/ml penicillin, 100 μ g/ml streptomycin, and 50 μ g/ml gentamycin sulfate at 37 °C with 5% CO₂. U937 cells were cultured in RPMI 1640 medium (pH 6.8). Media were supplemented with 10% FBS and antibiotics containing 50 IU/ml penicillin G and 50 μ g/ml streptomycin. The cells were incubated at 37 °C in a humidified atmosphere containing 5% CO₂ and subcultured every 72 h using an inoculum of 5 \times 10⁵ cells/ml. NHBE cells were cultured under air-liquid interface (ALI) as described previously

(62, 63). Cultures were grown at ALI for 12 days before the media were removed and replaced with media containing 2 nM (30 ng/ml) IL-13 and incubated for 72 h. Cells were tested and authenticated periodically and before each experiment both by monitoring cellular morphology at regular intervals by comparative microscopic observation using both high and low culture densities and by evaluating cellular growth analysis by checking proliferation and growth by standard MTT assay.

Isolation of human monocytes

Human peripheral blood monocytes (PBM) were isolated either by separation of mononuclear cells followed by adherence to BCS-coated flasks (40) or by Ficoll-Hypaque sedimentation followed by countercurrent centrifugal elutriation (64, 65). PBM purified by these two methods were identical in response to IL-13 and consistently >95% CD14⁺. These studies complied with all relevant guidelines and institutional policies regarding the use of human subjects.

Immunoprecipitation and immunoblotting

PBM were routinely treated with IL-13 (2 nM) for various time intervals. (This dose was chosen because it demonstrated comparable 15-LO induction in monocytes in numerous previous studies performed by our group.) Total and postnuclear extracts were prepared by previously published protocols (11, 66). After determining the protein concentration using the Bradford reagent from Sigma (catalog no. B6916), lysate proteins (50 µg/well) were resolved by 8–10% SDS-PAGE and subjected to immunoblotting as described previously (15). 15-LO protein was detected on Western blottings following a previously described protocol (40). Immunoprecipitation experiments were performed according to our previously published method (14) using prewashed Sepharose-protein G beads (20–50 µl of packed beads per volume/ml of extract) (Roche Diagnostics, Mannheim, Germany) at 4 °C overnight. The beads were washed three times with lysis buffer, and the immune complexes were collected. Immune complexes were released by boiling the beads in SDS sample buffer and were then subjected to Western blot analysis as described above. Immunoblots were stripped and reprobed to assess equal loading according to our previously published protocol (11).

RNA extraction and real-time RT-PCR

Monocytes (5×10^6 in 2 ml of 10% BCS/DMEM) were plated in six-well culture plates, treated with antisense or decoy ODN, and followed by treatment with IL-13 (2 nM) for 24 h. A549 and U937 cells were also treated similarly with the ODNs and incubated with IL-13 for the same time. In some groups, cells were directly treated with (13S)-HPODE/(13S)-HODE for the stipulated time period. Total cellular RNA was extracted using the RNeasy mini kit from Qiagen (Valencia, CA), and real-time quantitative RT-PCR was performed according to established protocol (12). The sequences of the primers used were as follows: 15-LO forward 5'-GCTGGAAGGATCTAGATGACT-3' and 15-LO reverse 5'-TGGCTACAGAGAATGACGTTG-3'; MAO-A forward 5'-GCCAAGATTCACCTCAGACAGAG-3' and MAO-A reverse 5'-TGCTCCTCACACCAGTTCTTCTC-3'. GAPDH was used as an internal control

with the primer sequences of forward 5'-CACCAACTGCTTAGCACCCC-3' and reverse 5'-TGGTCATGAGTCCCTCCACG-3'. 15-LO and MAO-A gene expression in primary monocytes and different cell lines were assessed by quantitative RT-PCR using SYBR Green on a 7500 Fast Real-time PCR system (Applied Biosystem).

DNA-binding activity of Stat1, Stat3, and Stat6

A TransAMTM Stat family kit (Active Motif) was used to evaluate the DNA-binding activity of Stat1, Stat3, and Stat6 according to the manufacturer's instructions. Briefly, nuclear extracts were incubated in a 96-well assay plate precoated with immobilized oligonucleotide containing the Stat consensus binding site (5'-TTCCCGGAA-3'). The active forms of Stat1, Stat3, and Stat6 contained in nuclear extracts specifically bind the oligonucleotide. The wild-type (WT) consensus oligonucleotide was provided with the kit as a competitor for Stat binding to monitor the specificity of the assay by preventing Stat binding to the probe immobilized on the plate. Conversely, the mutated consensus oligonucleotide was provided as a control and was expected to have a limited competition with the Stat consensus binding site. The detection of activated Stats (Stat1, Stat3, and Stat6) was carried out with specific Stat1 and Stat3 primary antibodies (supplied by the kit) and Stat6 rabbit polyclonal antibody (from Pharmingen) and an HRP-conjugated secondary antibody supplied in the kit. The detection of activated Stats was carried out by monitoring the colorimetric readout at 450 nm with a reference wavelength of 655 nm using a SynergyTM HT multimode microplate reader from Biotek. For competitive binding experiments, different oligonucleotides corresponding to the cognate Stat-binding sites (as predicted by Genomatix) in the context of 15-LO promoter-flanking sequences (StatX BS-15LO (oligonucleotides corresponding to the cognate Stat-binding site; StatX binds Stat1, Stat3, or Stat6) and Stat6 BS-15LO (oligonucleotides corresponding to one of the cognate Stat6-binding sites)) were used in this assay. The single-stranded sequences of these competitor ODNs were as follows: StatX BS-15LO sense, 5'-GAATGTACCTTCCCTCAAATGCCAC-3'; Stat6 BS-15LO sense, 5'-AGACTTTCCTGAGAAACCGGAGGT-3'. As a control competitor, we used the consensus Stat-binding site in the context of the same flanking sequences present in StatX BS-15LO (StatX BSC-15LO). The sequence of the sense strand of this control competitor (StatX BSC-15LO sense) was 5'-GAATGTACCTTCCCGGAATGCCAC-3'. As a noncompetitor, a mutated sequence of the cognate Stat-binding site in the context of the same flanking sequences present in StatX BS-15LO (StatX BS MT-15LO) was used in this assay. The sequence of the sense strand of this noncompetitor (StatX BS MT-15LO) was 5'-GAATGTACCGACGGCAGATGCCAC-3'. All of these ODNs were purchased from Integrated DNA Technologies (Coralville, IA).

ELISA to quantitate the DNA-binding activity of EGR1

A transcription factor ELISA kit from Panomics (Panomics, Santa Clara, CA) was used to assess the binding activity of EGR1 according to the manufacturer's instructions. In brief, activated EGR1 molecules from nuclear extracts bound to an EGR1 con-

Regulation of MAO-A in IL-13-activated cells

sensus binding site (EGR1 probe, 5'-GCGGGGCG-3') on a biotinylated oligonucleotide were immobilized on a streptavidin-coated 96-well assay plate. The EGR1, bound to the oligonucleotide, was detected by an antibody against EGR1, followed by an HRP-conjugated secondary antibody reaction with the TMB substrate to provide a colorimetric readout that was taken at 450 nm.

TransAMTM CREB activation assay

A TransAMTM CREB kit from Active Motif (Carlsbad, CA) was used to evaluate the cAMP-responsive element (CRE) promoter-binding activity of activated (phosphorylated) CREB according to the manufacturer's instructions. Nuclear extracts were incubated in a 96-well assay plate precoated with immobilized oligonucleotide containing the CRE promoter site (5'-TGACGTCA-3'). The detection of activated CREB was carried out with a specific pCREB primary antibody (1:500 dilution in 1× antibody binding buffer (supplied as a component by the kit)) and an HRP-conjugated secondary antibody. After incubation with the developing solution for the recommended time, the reaction was stopped, and the colorimetric readout was taken at 450 nm.

DNA-binding activity of PPAR γ

A TransAMTM kit (Active Motif) was used to evaluate the DNA-binding activity of PPAR γ according to the manufacturer's instructions. Briefly, nuclear extracts (10 μ g) were incubated in a 96-well assay plate precoated with immobilized oligonucleotide containing the PPRE (5'-AACTAGG-TCAAAGGTCA-3'). Activated PPAR γ (after treatment with rosiglitazone or IL-13) specifically binds the oligonucleotide. The detection of activated PPAR γ was carried out with a specific primary antibody and an HRP-conjugated secondary antibody supplied in the kit. The detection of activated PPAR γ was carried out by monitoring the colorimetric readout at 450 nm with a reference wavelength of 655 nm using a SynergyTM HT multimode microplate reader from Biotek. All the data shown represent the amount of activated PPAR γ in arbitrary units.

Monitoring of Sp1 DNA-binding

Monitoring of Sp1 activity was performed by an ELISA-based assay using a TransAMTM kit (Active Motif) to evaluate the DNA-binding capacity of Sp1 transcription factor according to the manufacturer's instructions. Briefly, nuclear extracts (5 μ g) were incubated in a 96-well assay plate precoated with immobilized oligonucleotide containing the Sp1 consensus binding site (5'-GGGGCGGGG-3'). Activated Sp1 (after treatment with IL-13) specifically binds the oligonucleotide. The detection of activated Sp1 was carried out with a specific primary antibody and an HRP-conjugated secondary antibody supplied in the kit. The detection of activated Sp1 was carried out by monitoring the colorimetric readout at 450 nm as described earlier. For competitive binding experiments, different oligonucleotides corresponding to the cognate Sp1-binding sites (as predicted by Genomatix) in the context of MAO-A promoter flanking sequences (Sp1 BS1-MAO-A (oligonucleotides corresponding to the cognate Sp1-binding site 1 located in the MAO-A promoter) and Sp1 BS2-MAO-A (oligonucleotides

corresponding to another cognate Sp1-binding site 2 in the MAO-A promoter)) were used in this assay. The single-stranded sequences of these competitor ODNs were as follows: Sp1 BS1-MAO-A sense, 5'-AGCCCCGGGGCGGAGCCGATCCTT-3'; and Sp1 BS2-MAO-A sense, 5'-CGCCCAGGGGCGGAGCTGATGTTT-3'. As a control competitor, we used the consensus Sp1-binding site in the context of the same flanking sequences present in Sp1 BS2-MAO-A (Sp1 BS2C-MAO-A). The sequence of the sense strand of this control competitor (Sp1 BS2C-MAO-A sense) was 5'-CGCCCAGGGGCGGGGCTGATGTTT-3'. As a noncompetitor, a mutated sequence of the cognate Sp1-binding site in the context of the same flanking sequences present in Sp1 BS2-MAO-A (Sp1 BS2-MT-MAO-A) was used in this assay. The sequence of the sense strand of this noncompetitor was 5'-CGCCCATTGCCCAAGCTGATGTTT-3'. All of these ODNs were supplied by Integrated DNA Technologies.

Treatment of monocytes and A549 and U937 cells with 15-LO and MAO-A antisense ODNs

15-LO antisense and sense ODNs were obtained from Invitrogen-Life Technologies, Inc., and handled according to the manufacturer's instructions. The 15-LO antisense ODN sequence was 5'-CCTGCACAGAGATCCAGTTGC-3'. A complementary 15-LO sense ODN sequence was used as a control. 15-LO antisense or sense ODNs (5 μ M) were boiled for 2–3 min and then cooled at room temperature before being added to human monocytes (5 × 10⁶ in 2 ml of 10% BCS/DMEM) and A549 and U937 cells. To check the effect of 15-LO antisense ODN on 15-LO protein expression, IL-13 (2 nm) was added to the appropriate samples 2 h after the antisense treatment. Cells were allowed to incubate at 37 °C and were re-fed with 15-LO sense and antisense ODNs (5 μ M) after 24 h. Cells were then harvested and assayed for silencing 48 h after 15-LO antisense treatment. For real-time PCR experiments with the 15-LO antisense ODNs, cells were treated with 15-LO sense or antisense ODNs (5 μ M) for a total period of 48 h with one re-feeding after 24 h prior to the stimulation with IL-13 for 24 h.

The sequences of the MAO-A antisense and sense ODNs are as follows: MAO-A, antisense 5'-ATTTGTTCAGCATGTTGAGCC-3', and MAO-A sense, 5'-GGCTCAACATGCTGACAAAT-3'.

For MAO-A sense and antisense treatment, cells were pretreated with MAO-A sense or antisense (AS) ODN (10 μ M) for 2 h prior to IL-13 addition and then re-fed with 10 μ M ODNs after 24 h and incubated for another 24 h before harvesting the cells. For the transfection control, cells were incubated with the transfection reagent alone for 48 h. All ODNs were end-modified (phosphorothioated, three bases at the 5' and 3' ends) to limit DNA degradation, and all were HPLC-purified before use (Invitrogen).

Transfection of Egr-1 and CREB decoy and scrambled decoy ODNs into monocytes

Double-stranded decoy ODNs containing the conserved promoter-binding site of the CREB, Egr-1, and a scrambled sequence were prepared from complementary single-stranded phosphorothioate-modified oligonucleotides ordered from

Invitrogen by melting at 95 °C for 5 min, followed by a cool-down phase for overnight. Human monocytes (5×10^6 cells/well in 2 ml of 10% BCS/DMEM) were plated in six-well culture plates overnight. Cells were then transfected with decoy ODN at a 2 μM concentration as indicated with Superfect Transfection Reagent (Qiagen, Valencia, CA) according to the manufacturer's instructions for 24 h. Monocytes were then incubated in the absence or presence of 2 nM IL-13 for another 24 h for MAO-A mRNA quantification or 48 h for MAO-A protein detection. The single-stranded sequences of the decoy ODNs were as follows: CREB (consensus): sense, 5'-AGAGATTG-CCTGACGTCAGAGAGCTA-3'; Egr-1 (consensus): sense, 5'-CCCGGCGCGGGGGCGATTTTCGAGTC-3'; scrambled: sense, 5'-AACAGAAGCCAGGAACCCTCCTCT-3', adapted from Grote *et al.* (67).

Transfection of Stat1, Stat3, and Stat6 decoy and mismatched/scrambled ODNs into primary monocytes and A549 cells

The phosphorothioated ODNs used for Stat1, Stat3, and Stat6 decoys were purchased from Invitrogen. These decoys were used in previous studies and shown to provide specific inhibition of Stat1, Stat3, and Stat6 activities (12, 68). The sequences for the decoys were 5'-ATATTCCTGTAAAGTG-3' and 3'-TATAAGGACATTCAC-5' for Stat1 decoy; 5'-ATATGGAGTAAGTG-3' and 3'-TATAACCTCATTAC-5' for the mismatched Stat1 decoy; 5'-GATCCTTCTGGGAATTCCTAGATC-3' and 3'-CTAGGAAGACCCTTAAGGATCTAG-5' for the Stat3 decoy; 5'-GATCCTTCTGGGCCGTCTAGATC-3' and 3'-CTAGGAAGACCCGGCAGGATCTAG-5' for the mismatched Stat3 decoy; 5'-GATCAAGACCTTTTCCCAAGAAATCTAT-3' and 3'-CATGTTCTGGAAAGGGTTCTTTAGATA-5' for Stat6 decoy; and 5'-CGAAATTCGTTAAATCACTAGCTTACC-3' and 3'-GCTTTAAAGCAATTTAGTGATCGAATGG-5' for the scrambled decoy ODN for Stat6. Stat1, Stat3, and Stat6 decoy, mismatched decoy, and scrambled decoy ODN sequences were prepared by annealing the single-stranded phosphorothioate-modified ODNs as described previously (12, 68). Human monocytes and A549 cells were then transfected with decoy ODNs using Superfect Transfection Reagent (Qiagen, Valencia, CA) according to the manufacturer's instructions for 24 h. Monocytes, A549, and U937 cells were further incubated with IL-13 for another 24 h for MAO-A mRNA quantification or 48 h for either MAO-A protein or native MAO-A enzyme activity detection.

Native MAO-A activity assay

MAO-A activity was measured by a two-step bioluminescent assay method as described previously (1, 69) using a MAO-GLOTM assay kit from Promega (Madison, WI). The amount of signal (light intensity) generated was detected using a microplate luminometer (Multilabel Counter Victor3TM, PerkinElmer Life Sciences). Human recombinant MAO-A enzyme (Promega) was used as a positive control. The results are expressed as relative light units after the background was subtracted.

Intracellular ROS determination

The generation of intracellular ROS was measured using the ROS-sensitive fluorescent probe H₂DCFDA (5 μM). After incubation with the probe for 30 min, cells were removed from the media, scraped off in PBS, washed, and centrifuged. Cell pellet was resuspended in prewarmed PBS, and the fluorescence was read (excitation 495 nm; emission 525 nm) as described previously (1, 38, 70).

Amplex Red monoamine oxidase assay

This assay is based on the detection of H₂O₂ in an HRP-coupled reaction using Amplex Red as a sensitive and stable probe (for H₂O₂) and p-tyramine as a substrate. The fluorometric assay was carried out following the manufacturer's instructions. Each reaction contained 1 mM p-tyramine, 1 unit/ml HRP, and 200 μM Amplex Red reagent. Reactions were incubated at room temperature for 60 min (protected from light), and fluorescence was measured with a fluorescence microplate reader using excitation at 571 nm and emission at 585 nm.

Mannose receptor expression by FACS analysis

FACS analyses were performed to assess the expression of mannose receptor on the surface of monocytes. Monocytes were harvested from plates by incubating with cell dissociation buffer (Invitrogen) for 10 min at 37 °C and then washed in PBS. The cell pellet was resuspended in PBS, and then 2×10^6 cells were preincubated with 4% normal goat serum for 30 min at 4 °C. The cells were spun down and then resuspended in 4% normal goat serum in PBS and incubated with FITC-conjugated mouse anti-human CD206 (macrophage mannose receptor mAb, BD Biosciences) for 30 min at 4 °C according to a protocol supplied by the manufacturer. Finally, the cells were washed, resuspended in PBS, and then analyzed using a FAC-ScanTM (BD Biosciences). An appropriate nonspecific isotype antibody was used as a negative control.

Chemotaxis assay for primary monocytes

Monocyte migration was evaluated using a microchamber technique (45, 71). DMEM with 15% BSA was added to the lower compartment of the disposable 96-well chemotaxis chamber in a total volume of 29 μl . The cell suspension (50 μl of 2×10^6 cells/ml and 1×10^5 cells/well) was added to the upper compartment of the chamber. The two compartments were separated by a 5- μm pore size, polycarbonate, polyvinylpyrrolidone-free filter. The chamber was incubated at 37 °C with 10% CO₂ for 90 min. At the end of the incubation, the filter facing the upper compartment was scraped with a sponge and rinsed gently with PBS to remove all nonmigrated cells. The side of the filter with the migrated cells was fixed and stained with the Hema3 stain set. Migrated monocytes were counted in five high-power fields ($\times 400$) using a light microscope. All samples were tested in triplicate, and the data are expressed as the means \pm S.D.

In vitro transwell migration assay

Chemical inhibitors or antisense ODN-treated A549 cells were used for the transwell migration assay after IL-13 stimu-

Regulation of MAO-A in IL-13-activated cells

lation for a stipulated time period. For this assay, cells (1.5×10^5) were placed in the upper chamber of the cell culture inserts (catalog no. 353182, BD Biosciences) with 400 μ l of serum-free medium and were allowed to migrate for 5 h in response to complete medium (DMEM with 15% FBS, 600 μ l) placed in the bottom chamber of the 12-well transwell plates. Cells that migrated to the lower surface of the membrane were fixed and stained with Giemsa, and at least five independent microscopic fields were counted under microscope.

In vitro cytotoxicity assay

A549 cells (5×10^5 /group) were treated with DMSO and different doses of pharmacological inhibitors for 96 h. Media were then removed, and cells were washed with $1 \times$ PBS twice. 100 μ l of cell suspension from each group were seeded in a 96-well microtiter plate and incubated for 4 h. MTT reagent was then added in each well (final concentration of 0.5 mg/ml) and incubated for 3 h (in absence of light) at 37 °C in the presence of 5% CO₂, and the cell viability was investigated by using the EZcount™ MTT cell assay kit (HiMedia, Mumbai, India). The resultant formazan crystals were dissolved in 100 μ l of solubilizing solution (supplied in the kit), and the absorbance of this product was measured at 570 nm using an ELISA plate reader (MULTISKAN EX Microplate Reader, ThermoFisher Scientific, Waltham, MA) with the reference wavelength higher than 650 nm.

Data analysis

The number of experiments analyzed is indicated in each figure. Band intensities were quantified by densitometric analyses using a laser densitometer (Microtek ScanMaker 8700, Cerritos, CA) and the ImageJ software program. Differences among experimental groups (for dose responses) were analyzed using one-way ANOVA. The significance of observations was calculated using unpaired Student's *t* test analysis, and $p < 0.05$ was considered statistically significant.

Author contributions—S. D. and P. D. formal analysis; S. D., P. D., P. B., P. K., and M. K. investigation; V. P. Y., M. K. C., and A. B. conceptualization; S. K., M. K. C., and K. B. resources; K. B. writing-review and editing; A. B. supervision; A. B. funding acquisition; A. B. writing-original draft.

References

- Bhattacharjee, A., Shukla, M., Yakubenko, V. P., Mulya, A., Kundu, S., and Cathcart, M. K. (2013) IL-4 and IL-13 employ discrete signaling pathways for target gene expression in alternatively activated monocytes/macrophages. *Free Radic. Biol. Med.* **54**, 1–16 [CrossRef Medline](#)
- Gordon, S. (2003) Alternative activation of macrophages. *Nat. Rev. Immunol.* **3**, 23–35 [CrossRef Medline](#)
- Gordon, S., and Martinez, F. O. (2010) Alternative activation of macrophages. Mechanism and functions. *Immunity* **32**, 593–604 [CrossRef Medline](#)
- Mantovani, A., Sica, A., Sozzani, S., Allavena, P., Vecchi, A., and Locati, M. (2004) The chemokine system in diverse forms of macrophage activation and polarization. *Trends Immunol.* **25**, 677–686 [CrossRef Medline](#)
- Mosser, D. M., and Edwards, J. P. (2008) Exploring the full spectrum of macrophage activation. *Nat. Rev. Immunol.* **8**, 958–969 [CrossRef Medline](#)
- Conrad, D. J., Kuhn, H., Mulkins, M., Highland, E., and Sigal, E. (1992) Specific inflammatory cytokines regulate the expression of human monocyte 15-lipoxygenase. *Proc. Natl. Acad. Sci. U.S.A.* **89**, 217–221 [CrossRef Medline](#)
- Nassar, G. M., Morrow, J. D., Roberts, L. J., 2nd., Lakkis, F. G., and Badr, K. F. (1994) Induction of 15-lipoxygenase by interleukin-13 in human blood monocytes. *J. Biol. Chem.* **269**, 27631–27634 [Medline](#)
- Chaitidis, P., Billett, E. E., O'Donnell, V. B., Fajardo, A. B., Fitzgerald, J., Kuban, R. J., Ungethuen, U., and Kühn, H. (2004) Th2 response of human peripheral monocytes involves isoform-specific induction of monoamine oxidase-A. *J. Immunol.* **173**, 4821–4827 [CrossRef Medline](#)
- Chaitidis, P., O'Donnell, V., Kuban, R. J., Bermudez-Fajardo, A., Ungethuen, U., and Kühn, H. (2005) Gene expression alterations of human peripheral blood monocytes induced by medium-term treatment with the TH2-cytokines interleukin-4 and -13. *Cytokine* **30**, 366–377 [CrossRef Medline](#)
- Bhattacharjee, A., Pal, S., Feldman, G. M., and Cathcart, M. K. (2011) Hck is a key regulator of gene expression in alternatively activated human monocytes. *J. Biol. Chem.* **286**, 36709–36723 [CrossRef Medline](#)
- Roy, B., Bhattacharjee, A., Xu, B., Ford, D., Maizel, A. L., and Cathcart, M. K. (2002) IL-13 signal transduction in human monocytes: phosphorylation of receptor components, association with Jaks, and phosphorylation/activation of Stats. *J. Leukoc. Biol.* **72**, 580–589 [Medline](#)
- Xu, B., Bhattacharjee, A., Roy, B., Xu, H. M., Anthony, D., Frank, D. A., Feldman, G. M., and Cathcart, M. K. (2003) Interleukin-13 induction of 15-lipoxygenase gene expression requires p38 mitogen-activated protein kinase mediated serine 727 phosphorylation of Stat1 and Stat3. *Mol. Cell. Biol.* **23**, 3918–3928 [CrossRef Medline](#)
- Xu, B., Bhattacharjee, A., Roy, B., Feldman, G. M., and Cathcart, M. K. (2004) Role of protein kinase C isoforms in the regulation of interleukin-13-induced 15-lipoxygenase gene expression in human monocytes. *J. Biol. Chem.* **279**, 15954–15960 [CrossRef Medline](#)
- Bhattacharjee, A., Xu, B., Frank, D. A., Feldman, G. M., and Cathcart, M. K. (2006) Monocyte 15-lipoxygenase expression is regulated by a novel cytosolic signaling complex with protein kinase C δ and tyrosine-phosphorylated Stat3. *J. Immunol.* **177**, 3771–3781 [CrossRef Medline](#)
- Bhattacharjee, A., Mulya, A., Pal, S., Roy, B., Feldman, G. M., and Cathcart, M. K. (2010) Monocyte 15-lipoxygenase gene expression requires ERK1/2 MAPK activity. *J. Immunol.* **185**, 5211–5224 [CrossRef Medline](#)
- Yamamoto, S. (1992) Mammalian lipoxygenases: molecular structures and functions. *Biochim. Biophys. Acta* **1128**, 117–131 [CrossRef Medline](#)
- Wittwer, J., and Hersberger, M. (2007) The two faces of the 15-lipoxygenase in atherosclerosis. *Prostaglandins Leukot. Essent. Fatty Acids* **77**, 67–77 [CrossRef Medline](#)
- Serhan, C. N., Chiang, N., and Van Dyke, T. E. (2008) Resolving inflammation: dual anti-inflammatory and pro-resolution lipid mediators. *Nat. Rev. Immunol.* **8**, 349–361 [CrossRef Medline](#)
- Folcik, V. A., Nivar-Aristy, R. A., Krajewski, L. P., and Cathcart, M. K. (1995) Lipoxygenase contributes to the oxidation of lipids in human atherosclerotic plaques. *J. Clin. Invest.* **96**, 504–510 [CrossRef Medline](#)
- Cathcart, M. K., and Folcik, V. A. (2000) Lipoxygenases and atherosclerosis: protection versus pathogenesis. *Free Radic. Biol. Med.* **28**, 1726–1734 [CrossRef Medline](#)
- Kühn, H., and O'Donnell, V. B. (2006) Inflammation and immune regulation by 12/15-lipoxygenases. *Prog. Lipid Res.* **45**, 334–356 [CrossRef Medline](#)
- Singer, T. P., and Ramsay, R. R. (1995) Flavoprotein structure and mechanism 2. Monoamine oxidases: old friends hold many surprises. *FASEB J.* **9**, 605–610 [CrossRef Medline](#)
- Wouters, J. (1998) Structural aspects of monoamine oxidase and its reversible inhibition. *Curr. Med. Chem.* **5**, 137–162 [Medline](#)
- Scrutton, N. S. (2004) Chemical aspects of amine oxidation by flavoprotein enzymes. *Nat. Prod. Rep.* **21**, 722–730 [CrossRef Medline](#)
- Wang, C. C., Borchert, A., Ugun-Klusek, A., Tang, L. Y., Lui, W. T., Chu, C. Y., Billett, E., Kuhn, H., and Ufer, C. (2011) Monoamine oxidase A expression is vital for embryonic brain development by modulating developmental apoptosis. *J. Biol. Chem.* **286**, 28322–28330 [CrossRef Medline](#)
- Moskvitina, T. A., and Medvedev, A. E. (2001) Different sensitivity of mitochondrial and cytosolic monoamine oxidases to *in vivo* but not *in*

- in vitro* inhibition by specific irreversible inhibitors. *Med. Sci. Monit.* **7**, 17–19 [Medline](#)
27. Meyer, J. H., Ginovart, N., Boovariwala, A., Sagrati, S., Hussey, D., Garcia, A., Young, T., Praschak-Rieder, N., Wilson, A. A., and Houle, S. (2006) Elevated monoamine oxidase levels in the brain: an explanation for the monoamine imbalance of major depression. *Arch. Gen. Psychiatry* **63**, 1209–1216 [CrossRef Medline](#)
 28. Schwartz, T. L. (2013) A neuroscientific update on monoamine oxidase and its inhibitors. *CNS Spectr.* **18**, Suppl 1, 25–32 [CrossRef Medline](#)
 29. Naoi, M., Maruyama, W., Akao, Y., Yi, H., and Yamaoka, Y. (2006) Involvement of type A monoamine oxidase in neurodegeneration: regulation of mitochondrial signaling leading to cell death or neuroprotection. *J. Neural Transm. Suppl.* **71**, 67–77 [Medline](#)
 30. Ou, X. M., Chen, K., and Shih, J. C. (2006) Monoamine oxidase A and repressor R1 are involved in apoptotic signaling pathway. *Proc. Natl. Acad. Sci. U.S.A.* **103**, 10923–10928 [CrossRef Medline](#)
 31. Brunner, H. G., Nelen, M., Breakefield, X. O., Ropers, H. H., and van Oost, B. A. (1993) Abnormal behavior associated with a point mutation in the structural gene for monoamine oxidase A. *Science* **262**, 578–580 [CrossRef Medline](#)
 32. Shih, J. C., Chen, K., and Ridd, M. J. (1999) Role of MAO A and B in neurotransmitter metabolism and behavior. *Pol. J. Pharmacol.* **51**, 25–29 [Medline](#)
 33. Adeghe, E., and Parvez, H. (2004) The effect of diabetes mellitus on the morphology and physiology of monoamine oxidase in the pancreas. *Neurotoxicology* **25**, 167–173 [CrossRef Medline](#)
 34. Panagiotidis, G., Lindström, P., Stenström, A., and Lundquist, I. (1993) Glucose modulation of islet monoamine oxidase activity in lean and obese hyperglycemic mice. *Metabolism* **42**, 1398–1404 [CrossRef Medline](#)
 35. Bianchi, P., Kunduzova, O., Masini, E., Cambon, C., Bani, D., Raimondi, L., Seguelas, M. H., Nistri, S., Colucci, W., Leducq, N., and Parini, A. (2005) Oxidative stress by monoamine oxidase mediates receptor-independent cardiomyocyte apoptosis by serotonin and posts ischemic myocardial injury. *Circulation* **112**, 3297–3305 [CrossRef Medline](#)
 36. Kaludercic, N., Carpi, A., Menabò, R., Di Lisa, F., and Paolucci, N. (2011) Monoamine oxidases (MAO) in the pathogenesis of heart failure and ischemia/reperfusion injury. *Biochim. Biophys. Acta* **1813**, 1323–1332 [CrossRef Medline](#)
 37. Pchejetski, D., Kunduzova, O., Dayon, A., Calise, D., Seguelas, M. H., Leducq, N., Seif, I., Parini, A., and Cuvillier, O. (2007) Oxidative stress-dependent sphingosine kinase-1 inhibition mediates monoamine oxidase A-associated cardiac cell apoptosis. *Circ. Res.* **100**, 41–49 [CrossRef Medline](#)
 38. Coatrieux, C., Sanson, M., Negre-Salvayre, A., Parini, A., Hannun, Y., Itohara, S., Salvayre, R., and Auge, N. (2007) MAO-A-induced mitogenic signaling is mediated by reactive oxygen species, MMP-2, and the sphingolipid pathway. *Free Radic. Biol. Med.* **43**, 80–89 [CrossRef Medline](#)
 39. Wu, J. B., Shao, C., Li, X., Li, Q., Hu, P., Shi, C., Li, Y., Chen, Y. T., Yin, F., Liao, C. P., Stiles, B. L., Zhau, H. E., Shih, J. C., and Chung, L. W. (2014) Monoamine oxidase A mediates prostate tumorigenesis and cancer metastasis. *J. Clin. Invest.* **124**, 2891–2908 [CrossRef Medline](#)
 40. Roy, B., and Cathcart, M. K. (1998) Induction of 15-lipoxygenase expression by IL-13 requires tyrosine phosphorylation of Jak2 and Tyk2 in human monocytes. *J. Biol. Chem.* **273**, 32023–32029 [CrossRef Medline](#)
 41. Yakubenko, V. P., Hsi, L. C., Cathcart, M. K., and Bhattacharjee, A. (2013) From macrophage interleukin-13 receptor to foam cell formation: mechanisms for $\alpha M\beta 2$ integrin interference. *J. Biol. Chem.* **288**, 2778–2788 [CrossRef Medline](#)
 42. Yakubenko, V. P., Bhattacharjee, A., Pluskota, E., and Cathcart, M. K. (2011) $\alpha M\beta 2$ integrin activation prevents alternative activation of human and murine macrophages and impedes foam cell formation. *Circ. Res.* **108**, 544–554 [CrossRef Medline](#)
 43. Martinez, F. O., Gordon, S., Locati, M., and Mantovani, A. (2006) Transcriptional profiling of the human monocyte-to-macrophage differentiation and polarization: new molecules and patterns of gene expression. *J. Immunol.* **177**, 7303–7311 [CrossRef Medline](#)
 44. Wu, N., Gu, H. J., and Li, Q. (2010) Effects of antidiabetic drug metformin on the migration and invasion abilities of human pulmonary adenocarcinoma A549 cell line *in vitro*. *J. Thorac. Dis.* **2**, 76–80 [Medline](#)
 45. Carnevale, K. A., and Cathcart, M. K. (2001) Calcium-independent phospholipase A(2) is required for human monocyte chemotaxis to monocyte chemoattractant protein 1. *J. Immunol.* **167**, 3414–3421 [CrossRef Medline](#)
 46. Mishra, R. S., Carnevale, K. A., and Cathcart, M. K. (2008) iPLA2 β : front and center in human monocyte chemotaxis to MCP-1. *J. Exp. Med.* **205**, 347–359 [CrossRef Medline](#)
 47. Kundu, S., Roome, T., Bhattacharjee, A., Carnevale, K. A., Yakubenko, V. P., Zhang, R., Hwang, S. H., Hammock, B. D., and Cathcart, M. K. (2013) Metabolic products of soluble epoxide hydrolase are essential for monocyte chemotaxis to MCP-1 *in vitro* and *in vivo*. *J. Lipid Res.* **54**, 436–447 [CrossRef Medline](#)
 48. Cathcart, M. K., and Bhattacharjee, A. (2014) Monoamine oxidase A (MAO-A): a signature marker of alternatively activated monocytes/macrophages. *Inflamm. Cell Signal.* **1**, e161 [Medline](#)
 49. Chaitidis, P., Billett, E., Kuban, R. J., Ungethuem, U., and Kuhn, H. (2005) Expression regulation of MAO isoforms in monocytic cells in response to Th2 cytokines. *Med. Sci. Monit.* **11**, BR259–BR265 [Medline](#)
 50. Itoh, T., Fairall, L., Amin, K., Inaba, Y., Szanto, A., Balint, B. L., Nagy, L., Yamamoto, K., and Schwabe, J. W. (2008) Structural basis for the activation of PPAR γ by oxidized fatty acids. *Nat. Struct. Mol. Biol.* **15**, 924–931 [CrossRef Medline](#)
 51. Nagy, L., Tontonoz, P., Alvarez, J. G., Chen, H., and Evans, R. M. (1998) Oxidized LDL regulates macrophage gene expression through ligand activation of PPAR γ . *Cell* **93**, 229–240 [CrossRef Medline](#)
 52. Kliewer, S. A., Sundseth, S. S., Jones, S. A., Brown, P. J., Wisely, G. B., Koble, C. S., Devchand, P., Wahli, W., Willson, T. M., Lenhard, J. M., and Lehmann, J. M. (1997) Fatty acids and eicosanoids regulate gene expression through direct interactions with peroxisome proliferator-activated receptors α and γ . *Proc. Natl. Acad. Sci. U.S.A.* **94**, 4318–4323 [CrossRef Medline](#)
 53. Szanto, A., Balint, B. L., Nagy, Z. S., Barta, E., Dezso, B., Pap, A., Szeles, L., Poliska, S., Oros, M., Evans, R. M., Barak, Y., Schwabe, J., and Nagy, L. (2010) STAT6 transcription factor is a facilitator of the nuclear receptor PPAR γ -regulated gene expression in macrophages and dendritic cells. *Immunity* **33**, 699–712 [CrossRef Medline](#)
 54. Bouhlel, M. A., Derudas, B., Rigamonti, E., Dièvert, R., Brozek, J., Haulon, S., Zawadzki, C., Jude, B., Torpier, G., Marx, N., Staels, B., and Chinetti-Gbaguidi, G. (2007) PPAR γ activation primes human monocytes into alternative M2 macrophages with anti-inflammatory properties. *Cell Metab.* **6**, 137–143 [CrossRef Medline](#)
 55. Odegaard, J. I., Ricardo-Gonzalez, R. R., Goforth, M. H., Morel, C. R., Subramanian, V., Mukundan, L., Red Eagle, A., Vats, D., Brombacher, F., Ferrante, A. W., and Chawla, A. (2007) Macrophage-specific PPAR γ controls alternative activation and improves insulin resistance. *Nature* **447**, 1116–1120 [CrossRef Medline](#)
 56. Czimmerer, Z., Varga, T., Poliska, S., Nemet, I., Szanto, A., and Nagy, L. (2012) Identification of novel markers of alternative activation and potential endogenous PPAR γ ligand production mechanisms in human IL-4 stimulated differentiating macrophages. *Immunobiology* **217**, 1301–1314 [CrossRef Medline](#)
 57. Carroll, J. S., Liu, X. S., Brodsky, A. S., Li, W., Meyer, C. A., Szary, A. J., Eckhoute, J., Shao, W., Hestermann, E. V., Geistlinger, T. R., Fox, E. A., Silver, P. A., and Brown, M. (2005) Chromosome-wide mapping of estrogen receptor binding reveals long-range regulation requiring the forkhead protein FoxA1. *Cell* **122**, 33–43 [CrossRef Medline](#)
 58. Lefterova, M. I., Zhang, Y., Steger, D. J., Schupp, M., Schug, J., Cristancho, A., Feng, D., Zhuo, D., Stoeckert, C. J., Jr., Liu, X. S., and Lazar, M. A. (2008) PPAR γ and C/EBP factors orchestrate adipocyte biology via adjacent binding on a genome-wide scale. *Genes Dev.* **22**, 2941–2952 [CrossRef Medline](#)
 59. Wu, J. B., Yin, L., Shi, C., Li, Q., Duan, P., Huang, J. M., Liu, C., Wang, F., Lewis, M., Wang, Y., Lin, T. P., Pan, C. C., Posadas, E. M., Zhau, H. E., and Chung, L. W. (2017) MAOA-dependent activation of Shh-IL6-RANKL

Regulation of MAO-A in IL-13-activated cells

- signaling network promotes prostate cancer metastasis by engaging tumor-stromal cell interactions. *Cancer Cell* **31**, 368–382 [CrossRef Medline](#)
60. Lin, Y. C., Chang, Y. T., Campbell, M., Lin, T. P., Pan, C. C., Lee, H. C., Shih, J. C., and Chang, P. C. (2017) MAOA-A novel decision maker of apoptosis and autophagy in hormone refractory neuroendocrine prostate cancer cells. *Sci. Rep.* **7**, 46338 [CrossRef Medline](#)
61. Cao, H., Zhang, J., Liu, H., Wan, L., Zhang, H., Huang, Q., Xu, E., and Lai, M. (2016) IL-13/STAT6 signaling plays a critical role in the epithelial-mesenchymal transition of colorectal cancer cells. *Oncotarget* **7**, 61183–61198 [Medline](#)
62. Brown, C. D., Kilty, I., Yeadon, M., and Jenkinson, S. (2001) Regulation of 15-lipoxygenase isozymes and mucin secretion by cytokines in cultured normal human bronchial epithelial cells. *Inflamm. Res.* **50**, 321–326 [CrossRef Medline](#)
63. Zhao, J., Maskrey, B., Balzar, S., Chibana, K., Mustovich, A., Hu, H., Trudeau, J. B., O'Donnell, V., and Wenzel, S. E. (2009) Interleukin-13-induced MUC5AC is regulated by 15-lipoxygenase 1 pathway in human bronchial epithelial cells. *Am. J. Respir. Crit. Care Med.* **179**, 782–790 [CrossRef Medline](#)
64. Wahl, L. M., Katona, I. M., Wilder, R. L., Winter, C. C., Haraoui, B., Scher, I., and Wahl, S. M. (1984) Isolation of human mononuclear cell subsets by counterflow centrifugal elutriation (CCE). I. Characterization of B-lymphocyte-, T-lymphocyte-, and monocyte-enriched fractions by flow cytometric analysis. *Cell Immunol.* **85**, 373–383 [CrossRef Medline](#)
65. Wahl, S. M., Katona, I. M., Stadler, B. M., Wilder, R. L., Helsel, W. E., and Wahl, L. M. (1984) Isolation of human mononuclear cell subsets by counterflow centrifugal elutriation (CCE). II. Functional properties of B-lymphocyte-, T-lymphocyte-, and monocyte-enriched fractions. *Cell Immunol.* **85**, 384–395 [CrossRef Medline](#)
66. Rosen, R. L., Winestock, K. D., Chen, G., Liu, X., Hennighausen, L., and Finbloom, D. S. (1996) Granulocyte-macrophage colony-stimulating factor preferentially activates the 94-kD STAT5A and an 80-kD STAT5A isoform in human peripheral blood monocytes. *Blood* **88**, 1206–1214 [Medline](#)
67. Grote, K., Bavendiek, U., Grothusen, C., Flach, I., Hilfiker-Kleiner, D., Drexler, H., and Schieffer, B. (2004) Stretch-inducible expression of the angiogenic factor CCN1 in vascular smooth muscle cells is mediated by Egr-1. *J. Biol. Chem.* **279**, 55675–55681 [CrossRef Medline](#)
68. Wang, L. H., Yang, X. Y., Kirken, R. A., Resau, J. H., and Farrar, W. L. (2000) Targeted disruption of stat6 DNA-binding activity by an oligonucleotide decoy blocks IL-4-driven T(H)2 cell response. *Blood* **95**, 1249–1257 [Medline](#)
69. Valley, M. P., Zhou, W., Hawkins, E. M., Shultz, J., Cali, J. J., Worzella, T., Bernad, L., Good, T., Good, D., Riss, T. L., Klaubert, D. H., and Wood, K. V. (2006) A bioluminescent assay for monoamine oxidase activity. *Anal. Biochem.* **359**, 238–246 [CrossRef Medline](#)
70. Robbesyn, F., Garcia, V., Auge, N., Vieira, O., Frisach, M. F., Salvayre, R., and Negre-Salvayre, A. (2003) HDL counterbalance the proinflammatory effect of oxidized LDL by inhibiting intracellular reactive oxygen species rise, proteasome activation, and subsequent NF- κ B activation in smooth muscle cells. *FASEB J.* **17**, 743–745 [CrossRef Medline](#)
71. Falk, W., Goodwin, R. H., Jr., and Leonard, E. J. (1980) A 48-well microchemotaxis assembly for rapid and accurate measurement of leukocyte migration. *J. Immunol. Methods* **33**, 239–247 [Medline](#)